1-1-1985

Analysis of creep-carburization-oxidation test data on inconel 625 and pyrolytic graphite, including pertinent background studies

Catherine A. Bronski

***

ANALYSIS OF CREEP-CARBURIZATION-OXIDATION TEST DATA ON INCONEL 625 AND PYROLYTIC GRAPHITE, INCLUDING PERTINENT BACKGROUND STUDIES*

by

Catherine A. Bronski**
Northern Illinois University
De Kalb, Illinois

Dr. Ankur Purohit
Safety Research Experiment Facilities
Argonne National Laboratory

*Work performed at Argonne National Laboratory, a contract laboratory of the United States Department of Energy.

**Participant in the Spring 1980 Undergraduate Research Participation Program, January 14 - May 2, 1980. This program is coordinated by the Argonne Center for Educational Affairs.

ANALYSIS OF CREEP-CARBURIZATION-OXIDATION TEST DATA ON INCONEL 625 AND PYROLYTIC GRAPHITE, INCLUDING PERTINENT BACKGROUND STUDIES

TABLE OF CONTENTS

TABLE OF CONTENTS (Cont'd)

LIST OF ABBREVIATIONS AND ACRONYMS

AES	Auger Electron Spectroscopy
AGS	Annulus Gas System
ALIP	Annular Linear Induction Pump
ANL	Argonne National Laboratory
ATL	Advanced TREAT Loop
CA	Calibration Assembly
CCOT	Creep-Carburization-Oxidation Test
cfh	Cubic Feet per Hour
CGS	Cover Gas System
CMA	Cylindrical Mirror Analyzer
CMS	Conversational Monitor System
E/E	Electronic/Electrical Systems
ESCA	Electron Spectroscopy for Chemical Analaysis
HEED	High-Energy Electron Diffraction
keV	One Thousand (1000) Electron Volts
kV	One Thousand (1000) Volts
LASL	Los Alamos Scientific Laboratory
LEED	Low-Energy Electron Diffraction
MSS	Mechanical Support Systems
pre-CCOT	Pre-Creep-Carburization-Oxidation Test
psi	Pounds per Square Inch
SAREF	Safety Research Experiment Facilities
SEM	Scanning Electron Microscopy
TREAT	Transient Reactor Test Facility
TU	TREAT Upgrade

ACKNOWLEDGEMENTS

I wish to thank Mr. Jerry E. Baird for his assistance in the selection of my project last fall and for his constant support throughout the spring semester.

I am very grateful to the director of SAREF Projects, Mr. Earle V. Krivanec, and to the associate director, Mr. Ronald E. Timm, for their generosity in granting me the opportunity to work as a member of the SAREF team. Thanks to their guidance and the extensive patience of my immediate supervisor, Dr. Ankur Purohit, my stay at Argonne became a learning experience as well as an enjoyable one. Ms. Janet Balson was responsible for helping me to retain my sense of humor.

My thanks are also due Mr. Ed Davis for his technical assistance in the preparation of the diagrams contained in this report. Ms. Shirley Biocic helped me immensely by proofreading and typing this report.

I am also grateful to my professors at Northern Illinois University, who have given extensively of their time and effort to assist me in the clarification of my career goals.

Finally, I wish to thank my good friend Mr. Robert B. Killeen, Jr., whose confidence in my abilities motivated me to apply for acceptance into this program.

1.0 INTRODUCTION

This semester I was chosen by the Argonne National Laboratory Center for Educational Affairs as a participant in their Undergraduate Research Participation Program. For my semester project, I was assigned to the Safety Research Experiment Facilities Division (SAREF). SAREF's current task is the TREAT Upgrade Project. This project entails the design and modification of several aspects of the Transient Reactor Test Facility (TREAT). TREAT, a test fast breeder reactor located at the Idaho Argonne National Laboratory, has the capacity to expose breeder reactor fuel elements to transients (short bursts of high power from the reactor).

Breeder reactors are nuclear reactors that create more fuel than they burn. They offer an almost unlimited source of energy but are also perceived as possible sources of nuclear proliferation. The research in breeder reactors is continuing in order to retain this potentially invaluable energy option.

The TREAT Upgrade Project involves the modification of several aspects of the TREAT site and building, one of which is the reactor core. There are two design options available in the modification of the reactor core. In one, pyrolytic graphite is being tested as an insulator in conjunction with Inconel 625 as the cladding jacket. (The cladding is the metal jacket that encloses the fuel.) The other design option has no insulator. Tests were performed on the cladding material for the TREAT Upgrade fuel assembly. As the reactor core is heated, the cladding material is expected to undergo a carburization/oxidation process

near the end of its lifetime. A short term program has been designed to simulate these conditions in prototypic, scaled down fuel assemblies. This program has been identified as the Creep-Carburization-Oxidation Test (CCOT). The program objectives of CCOT involve two steps. The first of these is to effect carburization on the inner surfaces of the fuel assembly cladding and oxidation on the outer surfaces, at elevated temperatures, for times simulating service. The second objective is to determine compressive creep (slow permanent deformation) during the conditioning program.

In order to accomplish part of the above objectives, data was collected on the effects of carburization and oxidation using optical and scanning Auger electron examination and analysis. J. Balson (also an Undergraduate Research Participant) and I entered the project at this point. Our task during the past semester has been to quantify this raw data using appropriate formulations and then display the results using a subset of the Argonne Computer Conversational Monitor System (CMS). The subset system is known as Tellagraf. During the quantification process and the process of displaying the results, we continually gained new knowledge concerning the validity of our analyses. Our formulations and display techniques were accordingly adjusted several times to reflect our improved understanding of the analysis of the data.

The data being analyzed had been collected using optical and scanning Auger electron spectroscopic techniques. It was thus necessary to possess a thorough understanding of the Auger electron process in order to provide the most valid explanation of the raw data. This understanding of the Auger electron process was obtained by conducting

an extensive literary search of the subject and by assimilating the information gained into a detailed report of the process. The basic technique of Auger electron spectroscopy, the underlying physics of the technique, and a detailed description of the Auger process itself are some of the topics which are included in the section entitled "Auger Electron Spectroscopy" (appearing as Section 4.0 of this report).

In order to realize the value of surface analysis techniques such as Auger electron spectroscopy, one must obtain a comprehension of the role surfaces play, if any, in the behavior of solids. There are instances in which surfaces have been found to influence the behavior of the material as a whole. The various ways in which these effects occur have been studied by this author. The results of this study have been summarized and are included in Section 5.0 of this report.

Several methods of materials analysis exist in addition to Auger electron spectroscopy. These methods were considered carefully as possible options before Auger electron spectroscopy was selected as the technique used to obtain the Creep-Carburization-Oxidation Test data. Section 6.0 of this report summarizes some of the additional techniques available to the materials scientist, life scientist, chemist, or medical researcher. The final section of this report, Section 7.0, examines some of the modern applications of such analysis techniques in the fields of chemistry, medicine, and the life sciences.

2.0 TREAT UPGRADE (TU) AND TU-RELATED SUPPORT FACILITIES

2.1 Summary

The TREAT Upgrade Project is being undertaken to provide an increase in the capability for in-reactor testing at the Transient Reactor Test Facility (TREAT) in support of the fast reactor safety program. This upgrading action is composed of four principal elements:[1]

(1) the design and acquisition of a large test vehicle, called the Advanced TREAT Loop (ATL), and its associated systems which can accommodate test fuel conditions and configurations typical of fast breeder reactor designs,

(2) the design and acquisition of the support equipment required for the assembly, disassembly, checkout, operation, testing, handling, and transport of the ATL,

(3) the modifications of the TREAT reactor and associated systems to accommodate the operation of the ATL and meet the sample energy deposition requirements for the experiment,

(4) the modification of the TREAT site and buildings to provide the capability for handling the ATL, to accommodate the ATL support equipment, and to facilitate operations.

Two significant constraints are imposed on this upgrading action:[2]

(1) the current irradiation capabilities of the TREAT reactor shall not be degraded, and

(2) the functional utility of TREAT shall not be interrupted for

an extended period of time. In addition, a limited amount of space within the TREAT reactor building is to be reserved for the possible future placement of equipment associated with the performance of safety research experiments with gas-cooled test loops.

2.2 Overall Plant Modifications

The TREAT Upgrade Project includes all of the systems, services, and facilities necessary to permit the performance of safety-related, in-reactor experiments utilizing the ATL test vehicle at the TREAT facility. Accordingly, the project encompasses the following activities:(3)

(1) the modifications of the existing TREAT facility including:
   (a) the site,
   (b) the building,
   (c) the mechanical services,
   (d) the electrical services,
   (e) the reactor core, and
   (f) the reactor systems,
(2) the design and acquistion of the ATL and its associated systems, and
(3) the design and acquisition of the ATL support equipment.

2.3 The Advanced TREAT Loop Systems

The Advanced TREAT Loop Systems include the following units:(4)

(1) the Advanced TREAT Loop (ATL),
(2) the ATL Mechanical Support Sytems (MSS),
(3) the ATL Electronic/Electrical (E/E) Systems, and
(4) the Calibration Assembly (CA).

The Advanced TREAT Loop Systems are being designed and built as part of the TREAT Upgrade Project (TU) which is one of the SAREF projects.

2.3.1 The Advanced TREAT Loop

The Advanced TREAT Loop is a packaged, sodium-cooled loop which will be used to perform safety experiments with fast reactor fuel pins (either fresh or preirradiated) in the TREAT Upgrade reactor as part of the Safety Research Experiment Facilities (SAREF Program).

The ATL is 27 ft in length and weighs approximately 7200 lbs.(5) There are six main components in the loop.(6) These are primary and secondary containments, a test train, an annular linear induction pump (ALIP), a neutron filter and a heater assembly. Sodium is pumped down along the inside surface of the primary containment by the ALIP and flows up through the test bundle to the plenum (an enclosed space) at the top, simulating conditions in a fast reactor. The test fuel bundle and most of the experiment instrumentation are part of the test train. The test train for each experiment will be different. Insofar as practicable, the reference test train design provides the envelope (a set of limitations) for all test trains. Test trains are expected to be within this design envelope. The secondary containment supports the ALIP, neutron filter, and heater assembly, and it completely surrounds the primary containment.

2.3.2 The Advanced TREAT Loop Mechanical Support Systems

The Mechanical Support Systems include the Annulus Gas System (AGS), a system which provides a pressure regulated inert gas to the space between the primary containment and secondary containment, and the Cover Gas System (CGS) which allows for setting the loop plenum static pressure at operating conditions.

2.3.3 The Advanced TREAT Loop Electronic/Electrical Systems

The Advanced TREAT Loop Electronic/Electrical Systems provide electrical power supplies, instrumentation, and process equipment to control sodium flow and temperature. This is accomplished by controlling pump and heater voltages and by providing sensors and associated electronics and consoles for loop control, display, and operational data recording.

2.3.4 The Calibration Assembly

The Calibration Assembly (CA) is a unit which simulates that portion of the ATL which will exist in the fuel assembly region of the TREAT reactor. The CA does not contain sodium, but does incorporate calibration fuel and/or monitor wires and foils. The function of the CA is to provide a neutronics mockup of a specific ATL such that reactor tests may be performed.(7) For example, the CA is used for TREAT reactor power calibration runs and trial transients from which the neutronics characteristics of the ATL can be determined.

2.3.5 Observation of Fuel Motion

The TREAT facility currently provides the capability to observe fuel motion. This capability is provided by the hodoscope and other fuel motion detectors; these will remain in operation for ATL experiments.(8) The ATL will be designed to provide for good hodoscope performance. Neutron radiography at TU will also be utilized.

2.4 TREAT Reactor Core

The existing TREAT reactor core is air-cooled and uses UO_2-graphite fuel. The fuel for the modified assemblies is a UO_2-graphite matrix

of the type used in the existing TREAT reactor core. The uranium is enriched fully (about 93.5%)[9] in ^{235}U. Graphite-uranium fuel having higher concentrations of enriched uranium than in the present TREAT fuel is specified for the modified fuel assemblies in order to increase high-temperature experiment performance. This fuel type has the following advantages:[10]

(1) The high heat-absorbing capability of the graphite matrix provides an effective heat sink for transient-generated heat without dependence on air coolant during the transient.

(2) The excellent thermal-shock resistance of graphite will sustain the high rates of heat input.

The experience with the existing TREAT fuel assemblies containing a lower concentration of uranium and operating up to a peak temperature of 650°C has been excellent.[11] The modified TREAT fuel assemblies fit within the space envelope of the current TREAT fuel assemblies. The fuel assemblies are 4 in square by 9 ft long.[12] They consist of a 4 ft central section of fuel with a 2 ft graphite reflector section on each end.

The upgrading of the reactor core is accomplished by replacing the central core region of existing fuel assemblies with new assemblies which are capable of much higher peak temperatures (~900°C).[13] This higher temperature is achieved with correspondingly higher ^{235}U loadings that are varied from fuel rod column to fuel rod column.[14] A cross section of the modified zone of the core is shown in Figure 1.[15] Approximately 100 new fuel assemblies are required. In addition, some

ITEMS NO.	DESCRIPTION
1	FULL FUEL ASSY.
2	VIEWING SLOT ASSY.
3	CORNER FUEL ASSY.
4	PARTIAL FUEL ASSY.
5	HALF VIEWING SLOT ASSY.
6	
7	BORDER FUEL ASSY.
8	INSTRUMENTED FUEL ASSY.
9	INSTRUMENTED FUEL ASSY.

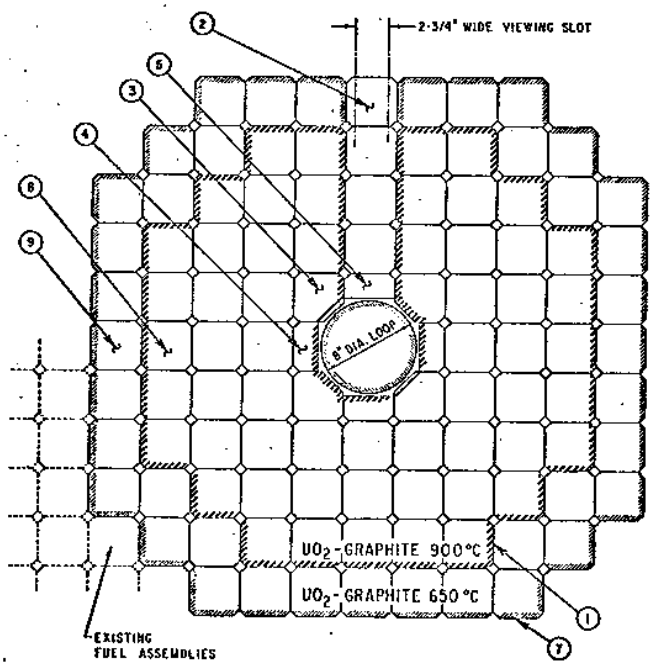

TREAT UPGRADE SECTION-CORE MAP

Figure 1

special assemblies are provided for the fuel motion viewing channels. The mechanical details of the new assemblies are maintained similar to those of the existing assemblies in order to preclude changes in fuel handling or core support equipment.(16)

The new assemblies use UO_2-graphite fuel.(17) Each fuel assembly will be a canned assemblage of UO_2-graphite fuel rods plus top and bottom graphite reflectors and necessary devices for holddown, establishment of an isolated environment for the fuel, and assembly handling.(18) The UO_2 will be fully enriched in ^{235}U. Since the uranium concentration is varied from fuel rod column to fuel rod column within each fuel assembly, each fuel assembly has an assigned core location and also an assigned orientation.(19)

The peak temperatures in the fuel rods in the modified fuel assemblies will be ~900°C.(20) The outer row of modified assemblies (shown in Figure 1) is derated in temperature to ~650°C to retard horizontal (radial) heat transfer from the modified zone and so prevent local overheating of the unmodified fuel assemblies just outside the modified zone. The design of the modified fuel assemblies inhibits overheating in the unmodified assemblies radially surrounding the modified zone, the ATL, and/or the core support structure.(21)

3.0 CAN ANALYSIS THROUGH USE OF THE CREEP-CARBURIZATION-OXIDATION TEST (CCOT)

3.1 Background

Modified TREAT fuel assemblies that can be taken to higher temperatures than the current TREAT assemblies are used in a major portion of the reactor core that is included within the central array of core assemblies (see Figure 1). In the reference design depicted in Figure 1, the assemblies in the inner portion of the modified zone have a peak operating temperature limit of ~900°C. Criteria for the selection of canning materials for the modified assemblies are: resistance to oxidation, strength at high temperature, and low neutron capture.(22) Materials that are being considered for the cans and end fittings are Inconel 625, along with both austenitic and ferritic stainless steels. The latter two are not studied in this report.

3.2 Introduction

The can provides a sealed environment for the modified fuel rods. Figure 1 diagrammatically shows about 100 cans in cross section. The central core region of the diagram depicts the modified fuel assemblies, which are capable of peak temperatures in the range of 900°C. These core assemblies are surrounded by an outer section of modified assemblies; these assemblies are capable of peak temperatures in the range of 650°C. The sheared corners of each fuel assembly in the reactor core combine with the sheared corners of the adjacent assemblies to form square coolant passages through the assembled core (see Figure 1).

The contents of the fuel assemblies are not shown in Figure 1;

Figure 2[23] represents an approximate enlargement of four of the can cross sections shown in Figure 1 (each of the four cans in Figure 2 would need its corners sheared off in order to provide a more accurate enlargement of the cans in Figure 1; this Figure 2 drawing is used for purposes of illustration only). The square graphite fuel rods contained within the fuel assemblies, as well as the four fuel assembly containment cans, are shown in Figure 2. A fuel can is simply a sheet of metal (such as Inconel 625) formed into a 4 in square piece, which is used to contain the fuel assembly. The cans used in the TREAT Upgrade reactor are 9 ft in length; the cans used for the collection of the Creep-Carburization-Oxidation Test (CCOT) data are 18 in length.[24] A photograph of a test can (4 in by 18 in) is shown in Figure 3.[25] The can shown in Figure 3 contains the fuel assembly; without the fuel assembly, the can forms a rectangular, hollow metal shell which is open at both ends.

3.3 Can Carburization/Oxidation

The TREAT Upgrade fuel assembly design being investigated by SAREF Projects calls for UO_2 dispersed in graphite and contained in Inconel 625 cladding material. At high operating temperatures, carburization as well as oxidation of the can's interior surface is expected to occur.[26] The extent of the carburization/oxidation process is dependent on the kinetics of the reactions involved. The operating lifetime of the can is primarily limited by the carburization process.[27] Carburization tends to decrease the ductility as well as lower the melting range of the cladding material. For temperatures less than 950°C, carburization is expected to be insignificant.[28] Above 950°C, the effects of carburization may be significant.[28] The micrograph labeled as Figure 4[29] was produced using a scanning electron

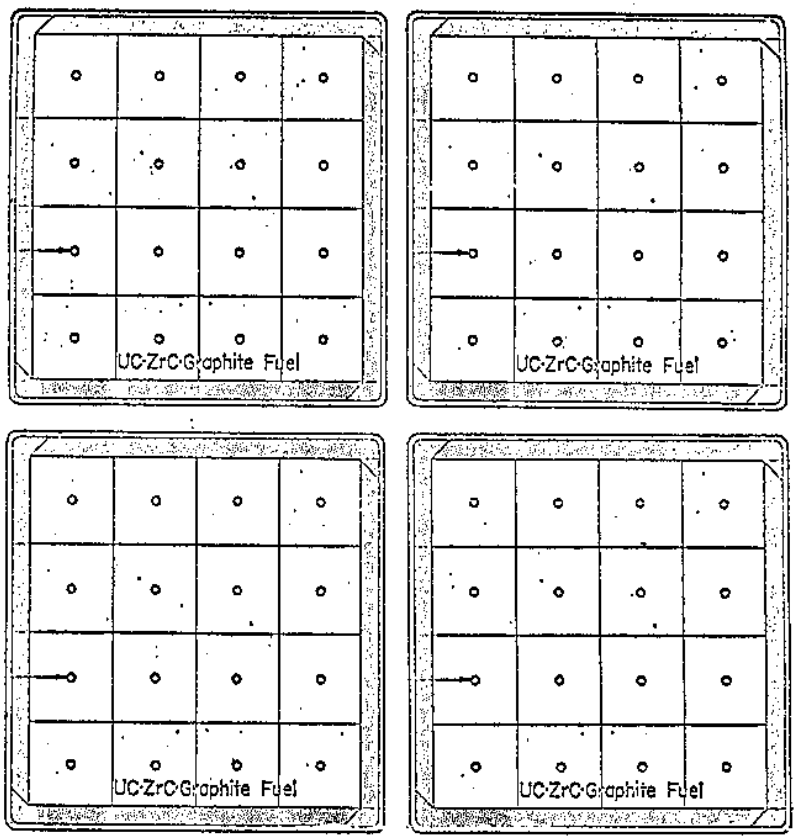
UC-ZrC-Graphite Fuel
UC-ZrC-Graphite Fuel
UC-ZrC-Graphite Fuel
UC-ZrC-Graphite Fuel

Figure 2

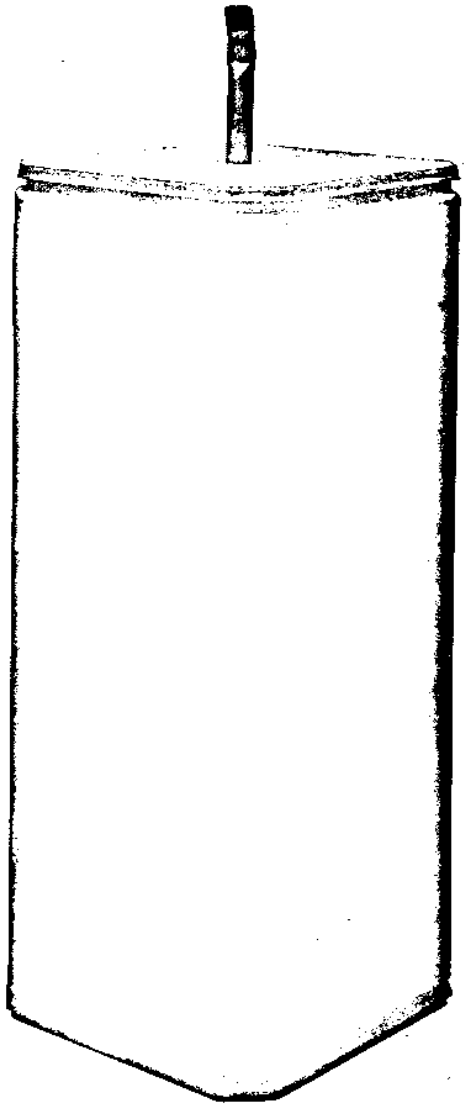

Figure 3

Figure 4

microscope (SEM). The material shown is from a section of a can used in one of the Creep-Carburization-Oxidation Tests (CCOT). (Since it was the second can produced, the can is arbitrarily known as CCOT-2). The can section shown had been heated to a temperature over 600°C prior to this micrograph being taken. The granular structures which nearly cover the Inconel 625 metal are believed to represent an oxide layer.[30] The oxidation in this case has most probably occurred through the formation of Cr_2O_3 on the Inconel surface. (The Inconel alloy contains the elements C, Fe, Ni, Mo and Cr, along with other elements present in trace amounts).[31] Near the center of the micrograph, thin black "channels" can be seen winding between the granular structures. These channels represent the grain boundaries of the Inconel 625.[32] Since these grain boundaries can be seen within the oxidized layer, the layer is known as a thin oxide layer. The magnification for this micrograph is ~2250x.

3.4 The Creep-Carburization-Oxidation Test (CCOT)

In order to establish the safety and the cost efficiency of the canning material Inconel 625 for the TREAT Upgrade Project, the CCOT program has been designed. It is necessary to determine the amount of carburization/oxidation which occurs at a heightened temperature, as a function of time at that temperature. Data is also sought on the depth of carburization/oxidation into the Inconel surface. It would also be beneficial to determine what chemical interactions, if any, occur between the carbides and oxides formed on the surface of the Inconel. It must be noted at this point that other aspects of the CCOT program will not be mentioned in detail in this report. Data collected on carburization/

oxidation amounts and carbide/oxide interactions will be correlated with other CCOT data at some future point in time. For example, the degree of carburization/oxidation will be compared with the mechanical properties of the can studied.

3.5 The Pre-Creep-Carburization-Oxidation Test (Pre-CCOT)

Prior to my involvement with SAREF Projects, it had been decided that a test run of the CCOT data collection program was needed. This test run, known as pre-CCOT, would be similar to the CCOT program, although not as extensive in testing as the CCOT. (It should be noted that the can size for the pre-CCOT was ⌀4 in square by ⌀6 in long).

The actual test on the pre-CCOT Inconel 625 cans was completed under the direction of K.V. Davidson at the Los Alamos Scientific Laboratory (LASL) in Los Alamos, New Mexico. This furnace test was made to investigate the possible reactions between Inconel 625 and high purity graphite.[33] The test was run at a nominal temperature of 1225K (950°C) for 187 h although the furnace was actually above 1175K (900°C) for 189 h.[34] The furnace used SiC resistance heating elements which heated an Inconel tube.[35] A sheet of Inconel 625 separated the furnace tube from the test cans. A thermocouple inside the furnace tube was used to measure and record the temperature directly over the test cans.

The two Inconel 625 test cans each contained three pieces of graphite rods which had been heat treated to 1550K.[36] The graphite pieces were 20.56 mm square by 152.4 mm long. The graphite was separated from the Inconel in one of the cans with a molybdenum foil.

The graphite pieces were machined to size. The cans containing the graphite pieces were welded closed in an atmosphere box containing argon. It was necessary to evacuate the cans for a few days as well as heat them slightly in order to reduce the helium in the pores of the graphite low enough to allow for leak checking. After pumping down to 4 μm and leak checking, the cans were filled with helium to a pressure of 1 psi absolute.(37)

The furnace took 8 h to reach the control temperature. The furnace retort was heated under vacuum to 720K, at which time the retort was backfilled with argon and the experiment was performed with 2 cfh flowing argon.(38)

After the heat treatment, it was observed that the cans had deformed inward due to the vacuum.(39) Some discoloration of the cans had also occurred. The thickness of the can assembly at various points was measured.

The welds were cut off one end of each can and the graphite pieces removed. A metallic deposit was present on the graphite wherever it was in contact with the can.(40) The can was sectioned to obtain metallographic samples. A SEM spectrographic X-ray analysis of the metallic layer on the graphite indicated a preponderance of chromium.(41) The Inconel surfaces had been changed by the corresponding depletion of chromium.

The outside surface of the Inconel cans was exposed to the argon atmosphere in the heat treating furnace and appeared to be slightly oxidized.(42) The graphite in the can with the molybdenum barrier

showed a metallic deposit only where the molybdenum foil did not form a tight seal.(43)

There appeared to have been a small reaction between the Inconel and the molybdenum and also between the molybdenum and the graphite.(44) The reaction area on the Inconel side of the molybdenum was examined by SEM spectrography; the results showed that there was some metallic transport across the interface.(45) The reactor area on the graphite side of the molybdenum was also examined, but only molybdenum was found; carbon cannot be determined by SEM spectrographic analysis, since its low atomic number provides little electron-scattering ability.(46)

In general, the test and examinations described above showed that the Inconel 625 and the high purity graphite will perform satisfactorily as materials for the test conditions defined.(47)

3.6 Analysis of Pre-Creep-Carburization-Oxidation Test Data (Pre-CCOT)

The role of the canning material in the TREAT Upgrade reactor core is an important one; as mentioned earlier (Section 3.4), the extent of carburization/oxidation may be related to the mechanical strength of the materials under investigation.(47) As a result of the possible potent consequences of the carburization/oxidation to the safety of the reactor, it was decided that the examinations performed at the Los Alamos Scientific Laboratory (LASL) (described in Section 3.5 above) gave data which needed to be expanded upon. The carburization/oxidation which seemed to have occurred in several places on the high purity graphite/Inconel 625 required a more extensive investigation. In studying carburization/oxidation which is produced subsequent to high temperature stress,

a detailed description of the amount of carburization/oxidation present in each atomic layer of the material under study is often useful. A surface analysis technique which only recently came into frequent use,[48] known as Auger electron spectroscopy (AES), was the method chosen for our atomic-level investigation of the carburization/oxidation processes under analysis. Section 4.0 of this report is an assimilation of knowledge gained by this author after an extensive literary search of the Auger electron process and Auger electron spectroscopy (AES). Section 4.0 includes an explanation of the basic Auger electron process (Section 4.3), as well as an account of the AES analysis technique (Section 4.4). The most common method of AES uses a cylindrical mirror analyzer; this method is explained in detail in Section 4.2. For those persons not familiar with AES and/or the Auger process, it may be useful at this point in time to review Section 4.0 in its entirety before continuing on in this report.

3.6.1 Depth Profiling Defined

In the pre-Creep-Carburization-Oxidation Test (pre-CCOT) program as well as the Creep-Carburization-Oxidation Test (CCOT) program, it was deemed necessary to determine the atom-layer by atom-layer elemental composition of the Inconel 625 canning material subsequent to the heat treatment described in Section 3.5. In this way, the degree of carburization/oxidation of the Inconel 625 could be determined as a function of the distance from the surface of the Inconel 625; a determination of the elemental composition as a function of the penetration depth into the material's surface is known as a depth profile chart. A depth profile chart may be obtained by using Auger electron spectroscopy in conjunction

with a sputter ion gun.[49] As explained further in Section 4.2, the sputter ion gun uses inert gas ion bombardment to erode contaminated layers from the specimen surface in a relatively controlled but nonetheless destructive fashion.[50] Used in this way, the sputter ion gun is turned on for only a few milliseconds before the Auger electron spectroscope is employed.[51] In addition to its role as a surface-cleaning tool, however, the sputter ion gun may also be used to acquire a depth profile chart. If the sputter ion gun's beam and the AES electron beam are both aimed at the focal point of the electron spectrometer, the elemental composition of the sample will be recorded as the ion gun continues to erode the surface atom-layer by atom-layer.[52] Sputtering rates of up to 3 Å/sec can be achieved for most materials using argon ions of 1,000-2,000 electron volts (1-2 keV).[53] Thus, by knowing the sputtering rate, one can obtain a depth profile chart.

3.6.2 Depth Profiling of Pre-Creep-Carburization-Oxidation Test (Pre-CCOT) Data

The sputtering rate of either 30 Å/min or 100 Å/min was used as a multiplication factor to determine the distance from the exposed Inconel 625 surface.[54] The sputtering rate for heat-treated Inconel 625 can be determined by first obtaining a sputtering rate for Inconel 625 which has not been heat-treated. The latter sputtering rate is known as the sputtering coefficient for the material in its as-processed state (untreated Inconel 625, in this case).[55]

The elemental composition data analyzed was accompanied by a time factor for each data point. By multiplying the time factor by the time in minutes, the distance from the exposed surface was obtained, in Angstroms.

The data to be analyzed by J. Balson and this author were presented to us in a form similar to that shown in Figure 5. The peak-to-peak amplitude intensity of the differential (see Figure 5, upper curve) is proportional to the amount of the element present.[56] Thus, it is a common practice in Auger electron spectroscopy to use the peak-to-peak signal strength in the derivative spectrum as a relative quantitative measure of elemental surface concentration.[57] By measurement of the peak-to-peak amplitude intensity it was then possible to use set formulations on the intensity values, and in so doing eventually obtain the approximate elemental composition of the sample.

Figures 6-9 inclusive illustrate several samples of the graphed results obtained from our analysis of the pre-Creep-Carburization-Oxidation Test data. The graphed results portray how the elemental concentration in the alloy varies with the distance from the exposed surface (i.e., the depth of penetration into the exposed surface), in 1000 Å. The graphed results of Specimen Can 1 are shown in Figure 6. Specimen Can 1 was heated for 187 h at 1225K (950°C)[58] as mentioned earlier in this report (Section 3.5). Figure 7 is a graph of the results obtained from Specimen 5-5; this specimen was heated for 1 hr at 1495K (1220°C).[59] A graph of the results obtained from Specimen 5-17 is shown in Figure 8. Specimen 5-17 was heat-treated for 4 h at 1495K (1220°C).[60] The specimen shown in Figure 9 (Specimen 5-21) was heated for 100 h at 1225K (950°C).

3.6.3 Display of Pre-Creep-Carburization-Oxidation Test (Pre-CCOT) Data

The data collected on the effects of carburization and oxidation using optical and scanning Auger electron examination needed analyzation

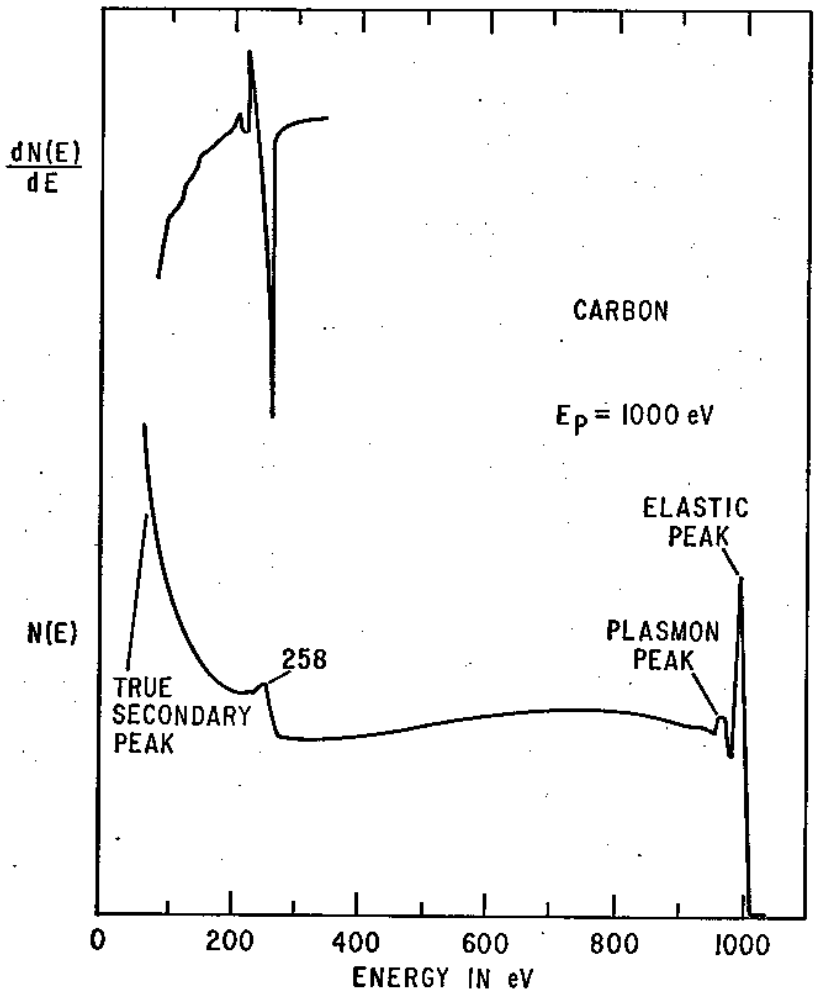
dN(E)
dE
CARBON
E_p = 1000 eV
ELASTIC
PEAK
N(E)
PLASMON
PEAK
258
TRUE
SECONDARY
PEAK
0
200
400
600
800
1000
ENERGY IN eV

Figure 5

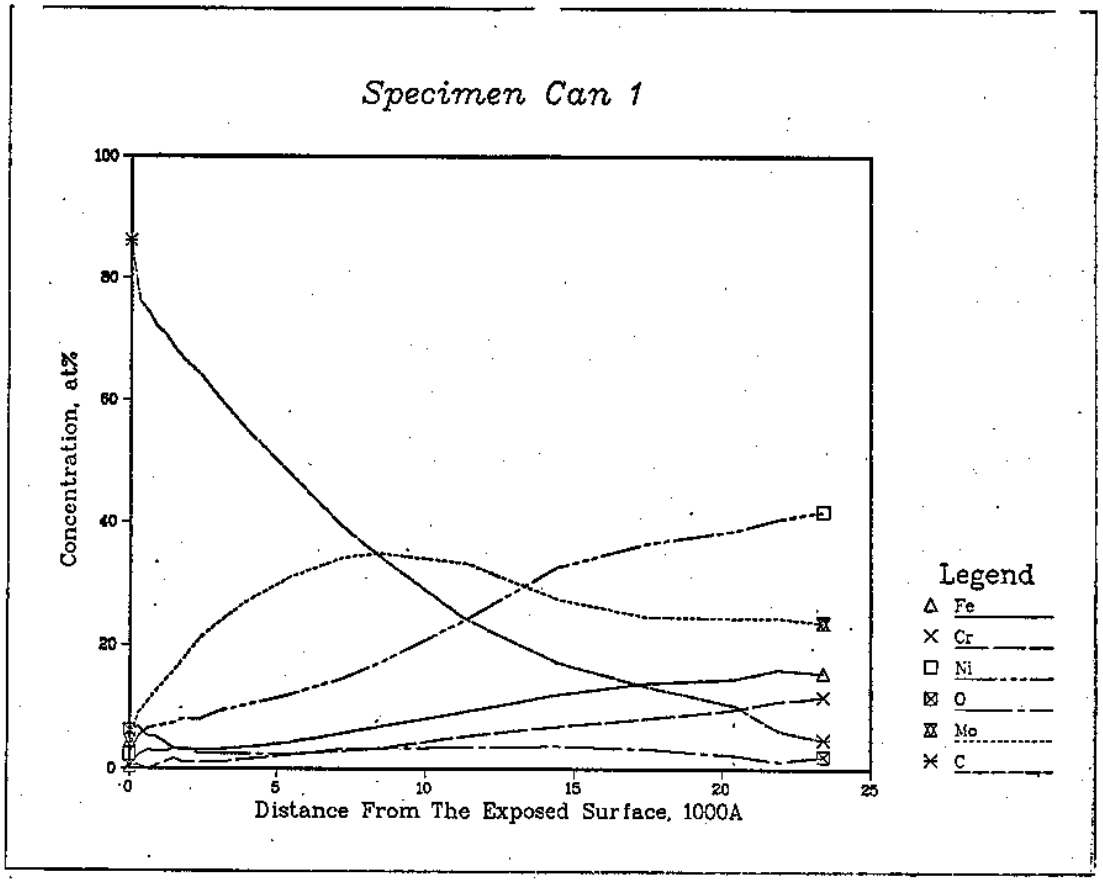
Specimen Can 1
Concentration, at%
100
80
60
40
20
0
0
5
10
15
20
25
Distance From The Exposed Surface, 1000A
Legend
Fe
Cr
Ni
O
Mo
C

Figure 6

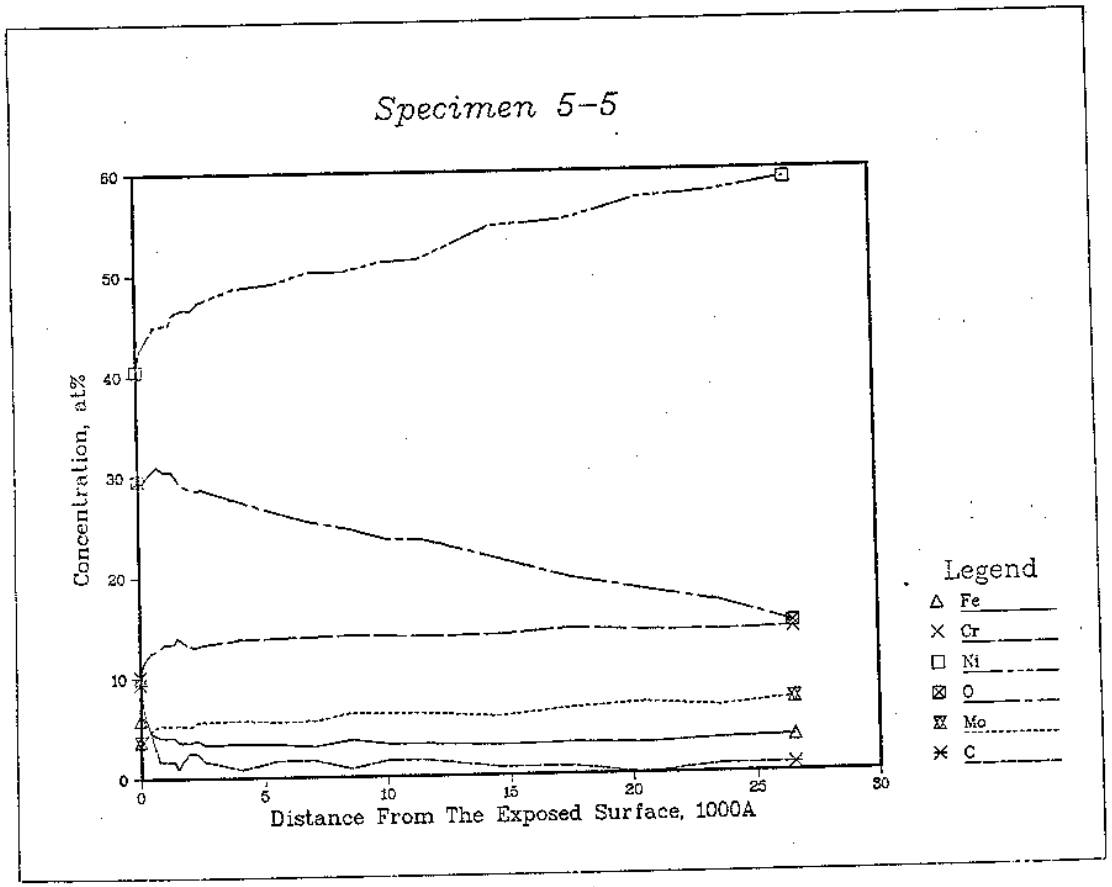
Specimen 5-5
Concentration, at%
60
50
40
30
20
10
0
0
5
10
15
20
25
30
Distance From The Exposed Surface, 1000A
Legend
Fe
Cr
Ni
O
Mo
C

Figure 7

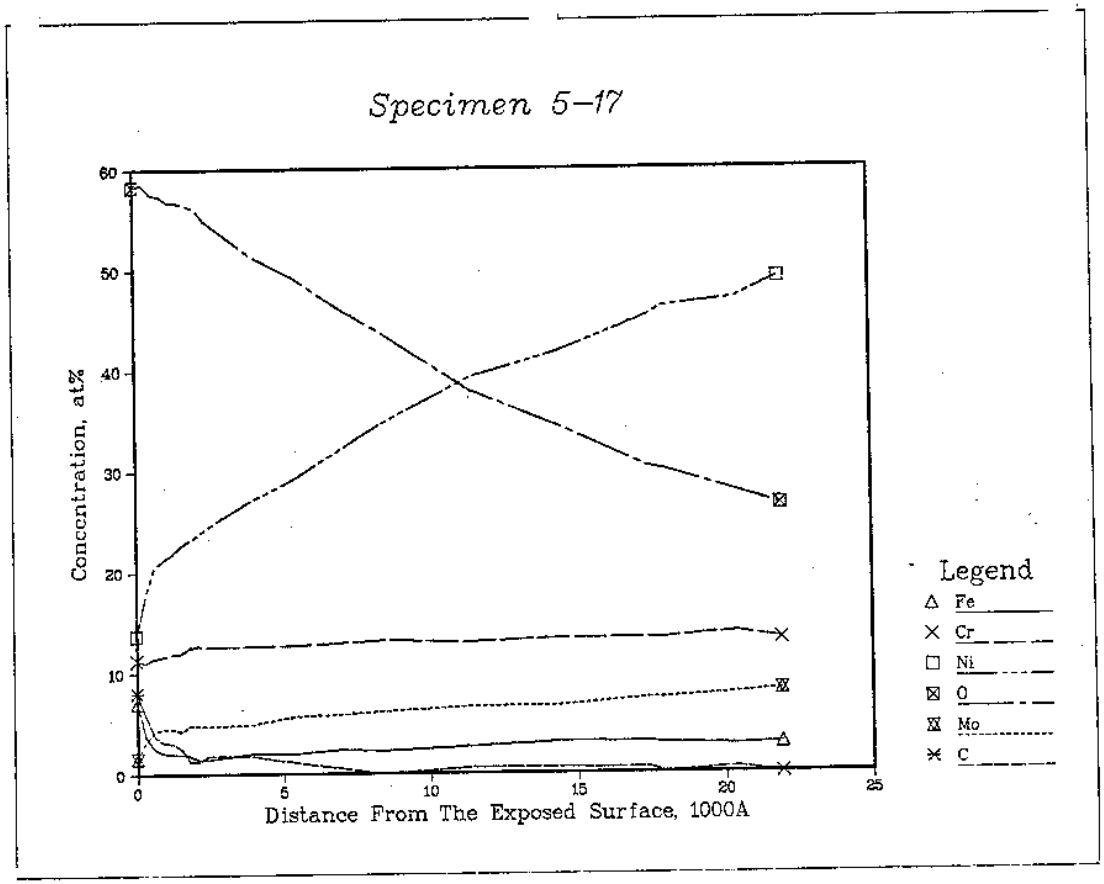
Specimen 5-17
Concentration, at%
Distance From The Exposed Surface, 1000A
0
10
20
30
40
50
60
0
5
10
15
20
25
Legend
Fe
Cr
Ni
O
Mo
C

Figure 8

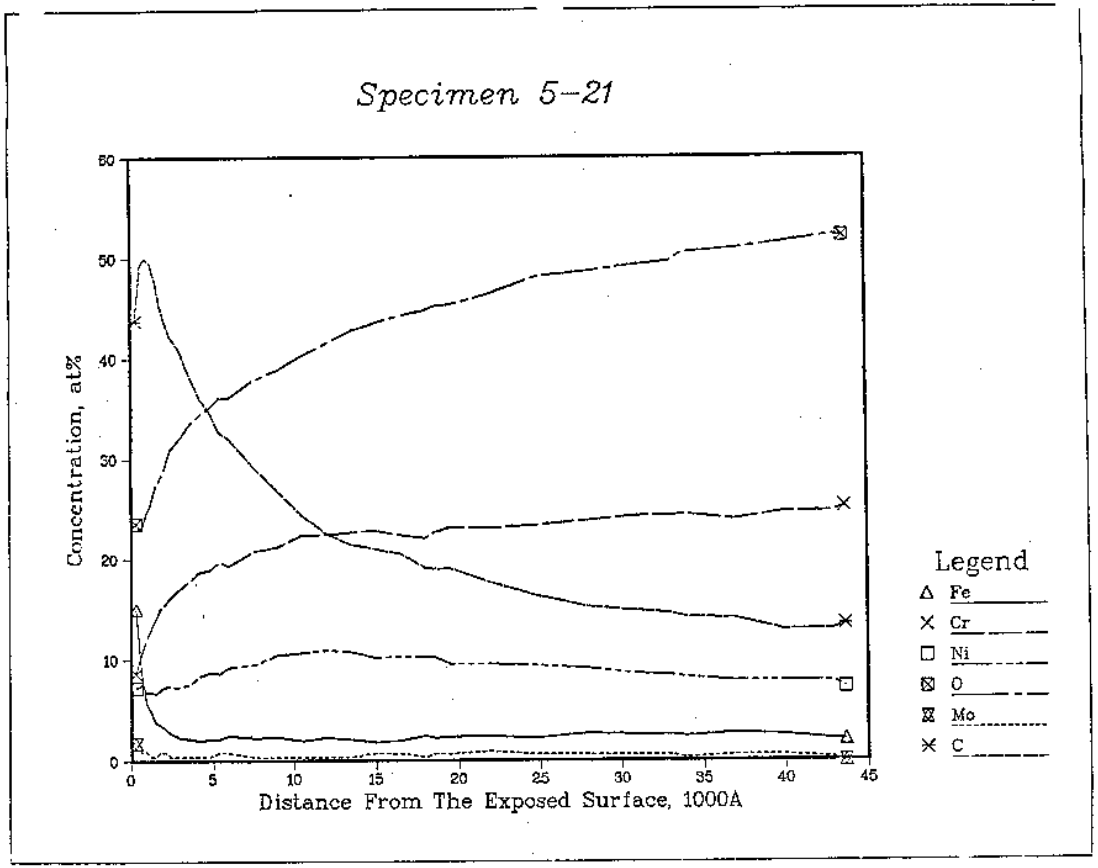
Specimen 5-21
Concentration, at%
Distance From The Exposed Surface, 1000A
0
10
20
30
40
50
60
0
5
10
15
20
25
30
35
40
45
Legend
Fe
Cr
Ni
O
Mo
C

Figure 9

in order for it to be of value. This raw data was quantified using appropriate formulations and the results displayed using a subset of the Argonne Computer Conversational Monitor System (CMS); this subset system is known as Tellagraf. Samples of the graphed results obtained through Tellagraf appear in Figures 6-9.

3.6.4 The Application of Set Formulations

Auger electron transitions require three electron levels; consequently, only those elements with atomic numbers greater than three can be detected.(62) The rate of core-level ionization is one of the key factors in Auger transition intensity and can be adjusted by varying the primary electron beam energy so that the relative KLL, LMM, and MNN intensities are altered (see Section 4.0).(63) The KLL Auger transitions are the most intense for low-atomic-number elements, while the LMM transitions increase in intensity with increasing atomic number, and subsequently the MNN transitions increase as well. By progressively using the KLL, LMM, and MNN series of Auger transitions, the elemental sensitivity variation across the periodic table can be held to a factor of less than fifty.(64)

A highly useful method for determining atomic concentrations makes use of the atomic KLL, LMM, and MNN transition intensities. Assuming that the transition intensities can be measured for the pure elements under a set of controlled conditions, the atomic concentration of element X can be expressed as:

$$C_X = (I_X/S_X)\Big/\sum_a (I_a/S_a),^{(65)}$$

where C_X = the atomic concentration of elemnent X,

I_X = the Auger transition intensity of element X (the measured peak-to-peak amplitude of element X), and

S_X = the relative sensitivity.

The intensity to sensitivity ratio is determined for each element ( ) in the sample. These values are then summated and the total is divided into the value obtained for element X.

In actuality, the sensitivity may be determined by either of two methods. In the first method, a standard of silver is used to determine the sensitivity of each element in the sample being analyzed. In the second method, established standards for each element have been used to determine the sensitivity of that element; these sensitivities are recorded in the Handbook of Physical Auger Elemental Energies.(66)

Due to the delicacy of the instrumentation and the number of electronic systems necessary for analysis, each Auger electron spectrometer varies slightly, depending on conditions of the sample and the condition of the equipment used. It is for this reason that Auger analysis for quantification is best performed through use of the first method mentioned.(67) In this method, standard samples of silver are run for analysis. By knowing the peak-to-peak amplitude of silver, the sensitivity of another element can be calculated, using the following equation:

$$S_X\,(Ep) = \left(A+B/A\right)\left(I_X/K_X I_{Ag}\right).\ (68)$$

In this equation:

Ep = the primary beam energy,

S_X = the relative sensitivity,

A and B = the chemical formula indices (obtained from a handbook),

K_X = a scale factor (obtained from a handbook),

I_X = the Auger transition intensity of element X (the measured peak-to-peak amplitude of element X), and

I_{Ag} = the Auger transition intensity of silver (the measured peak-to-peak amplitude of silver).

By knowing the relative sensitivity, the concentration in atom percent can be calculated. The formulations required for this operation can be obtained from the Handbook of Auger Electron Spectroscopy (see Reference 66).

It was only after the pre-CCOT data collection had taken place that the superior value of the first method was realized. Unfortunately, no alloy standards were run for the pre-CCOT data for this reason.

In order to compensate for the lack of alloy standards, the following assumptions and procedures were made. It was assumed that after a certain amount of sputtering time, the entire oxidized or carburized layer would be removed from the sample. It was also assumed that the analysis of the alloy Inconel 625 after removal of this oxidized or carburized layer would be equivalent to an analysis of pure alloy. In this way, the samples were interpreted backwards from the assumed location of the pure alloy. Since the concentration of elements in the pure alloy Inconel 625 is known, the values can be inserted for each element and the curves can be adjusted from the greatest sputter depth to the surface.

As mentioned earlier, when silver standards are not used (i.e., when the first sensitivity determination method is not followed), the elemental concentration can be calculated from the equation:

$$C_X = (I_X/S_X) \Big/ \sum_a (I_a/S_a).$$

Since six elements were present in the sample, the equation became very complex and tedious to perform. Much time was saved in performing the calculations on the data as a result of the development of a calculator program by J. Balson for the programmable calculators used. A flow chart depicting the steps of this program is given in Figure 10.(69)

It was decided that the pre-CCOT data obtained could be more easily analyzed and compared with other data if the pre-CCOT data concentrations were in weight percent rather than atom percent. To obtain the weight percent, the following equation was used:

$$W_X = A_X \cdot AW_X \Big/ \sum A\alpha \cdot AW_\alpha , \quad (70)$$

where W_X = the weight percent of the element X,

A_X = the atom percent of the element X,

AW_X = the atomic weight of the element X.

The multiplication of A by AW is determined for each element (α) in the sample; the values are summated and the total is divided into the value obtained for element X.

As a result of this adjustment, Figure 11 gives a preliminary evaluation of concentration in the Inconel 625 alloy for Specimen Can 1. Values given in the legend represent the weight percent at location A (this represents the alloy composition). Interpretation of the information at any other location requires linear extrapolation from point A along the appropriate curve. As stated earlier, this adjustment of concentration values is necessary due to a lack of alloy standards. In Figure 12 this linear extrapolation has been performed from point A along the appropriate curve for Specimen Can 1.

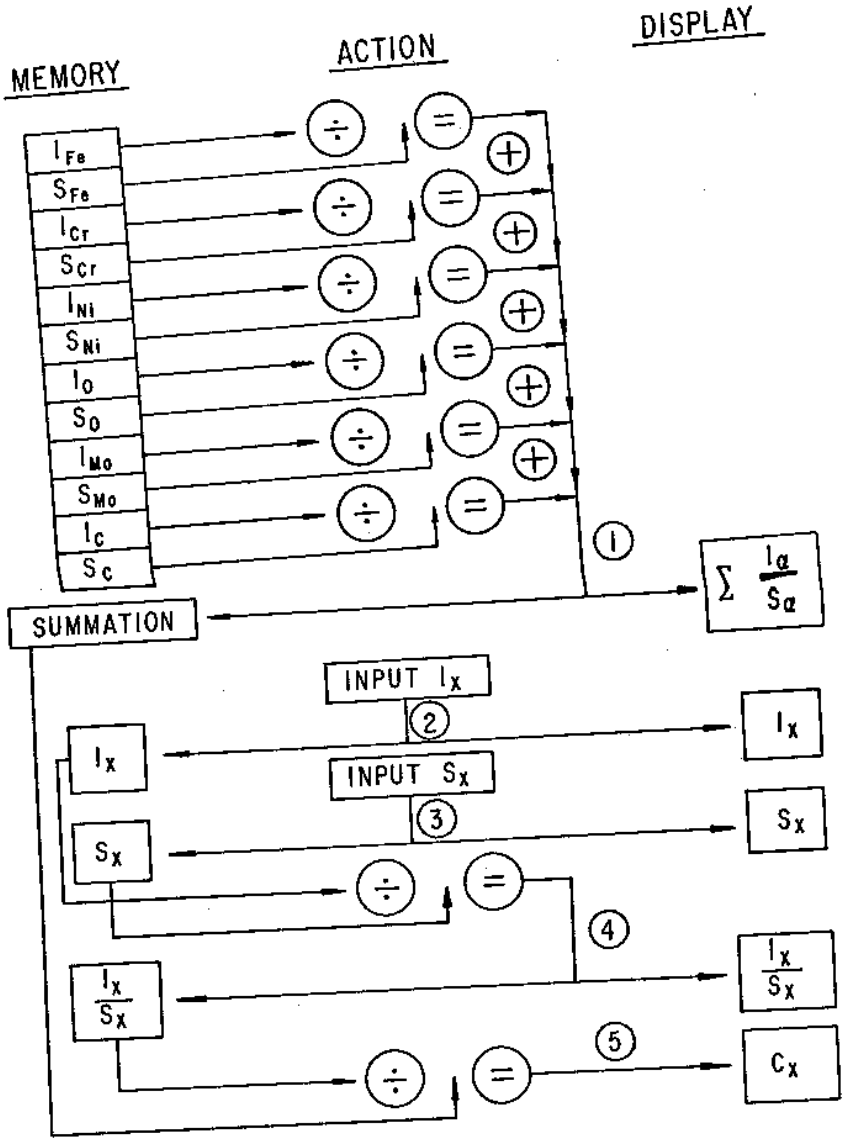
MEMORY
ACTION
DISPLAY
I_{Fe}
S_{Fe}
I_{Cr}
S_{Cr}
I_{Ni}
S_{Ni}
I_O
S_O
I_{Mo}
S_{Mo}
I_C
S_C
SUMMATION
①
$\sum \frac{I_\alpha}{S_\alpha}$
INPUT I_X
②
I_X
INPUT S_X
③
S_X
④
$\frac{I_X}{S_X}$
⑤
C_X

Figure 10

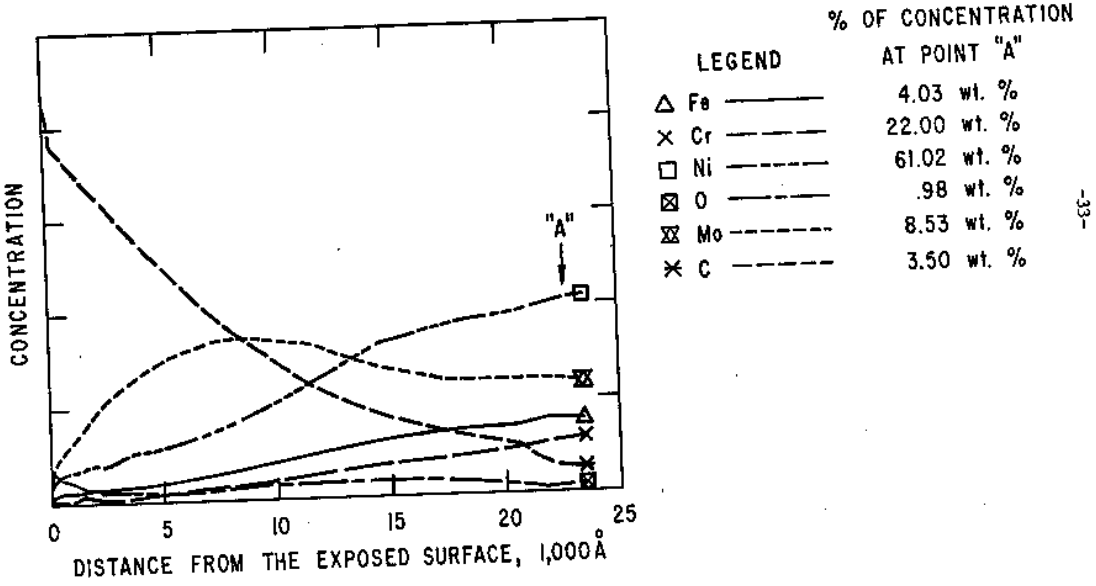
% OF CONCENTRATION
AT POINT "A"
LEGEND
Fe 4.03 wt. %
Cr 22.00 wt. %
Ni 61.02 wt. %
O .98 wt. %
Mo 8.53 wt. %
C 3.50 wt. %
"A"
CONCENTRATION
0
5
10
15
20
25
DISTANCE FROM THE EXPOSED SURFACE, 1,000 Å

Figure 11

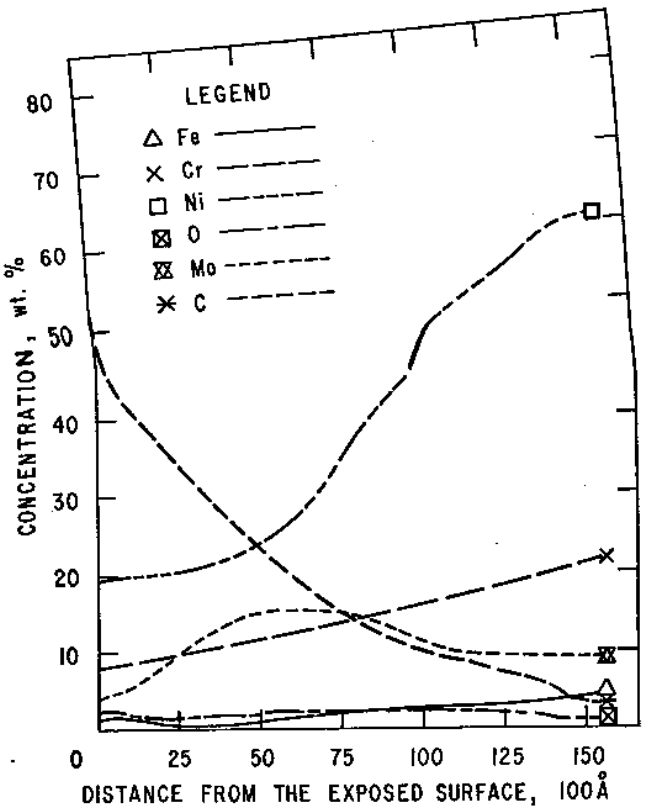
LEGEND
Fe
Cr
Ni
O
Mo
C
CONCENTRATION, wt. %
80
70
60
50
40
30
20
10
0
25
50
75
100
125
150
DISTANCE FROM THE EXPOSED SURFACE, 100Å

Figure 12

3.6.5 Conclusions

The results indicated that for the most part, on the carburization side of the specimens, chromium carbides were formed and, at higher temperatures, molybdenum carbides were also formed. On the oxidation side of the specimens, mostly chromium oxides and iron oxides were formed. As was mentioned earlier in this report, it is necessary to determine the amount of carburization present on the specimens before determining what factors (if any) carburization affects, and to what degree. An example of one such possible factor is mechanical strength; studies determining to what degree mechanical strength is affected by carburization (if at all) are yet to be done for the CCOT data.

As a whole, the material seemed to function adequately for the times and temperatures studied. Since the changes in the elemental composition of the specimens are now graphed as a function of sputtering time and/or penetration depth, future studies on the properties of the material as a whole can now be more easily correlated with the elemental composition changes.

4.0 AUGER ELECTRON SPECTROSCOPY

4.1 Summary

One of the most popular methods of surface analysis used today is Auger electron spectroscopy, also known as AES. Basically defined, AES is a relatively new analytical technique which provides a quantitative and qualitative analysis of the elements present in the outer four or five atomic layers of a non-volatile specimen surface.(71) The basic technique consists of bombardment of the surface with a beam of electrons in the range 1,000-5,000 electron volts. When an electron beam with this energy hits a specimen, the atoms of the specimen will emit additional electrons having energies characteristic of the emitting atoms. These additional ejected electrons are the Auger electrons. Analysis of the energies of these ejected Auger electrons and measurement of the current due to Auger electrons then provides analytical information necessary to determine surface elemental composition.(72) One main advantage of this technique is that it is non-destructive; in other words, the process will not erode the surface of the sample studied.(73)

4.2 The Cylindrical Mirror Analyzer

To proceed with a complete explanation of AES, it is first necessary to consider the details of the experimental scheme for detection of Auger electrons. Palmberg's diagram(74) of a cylindrical mirror analyzer (CMA) is depicted in Figure 13. The cylindrical mirror analyzer is the most common method used to perform Auger electron spectroscopy.(75) Following is a brief explanation of how the CMA works. Specimens (here depicted as five shaded boxes) are held by the carrousel target holder, which can be rotated in the direction of the arrow to facilitate analysis of the

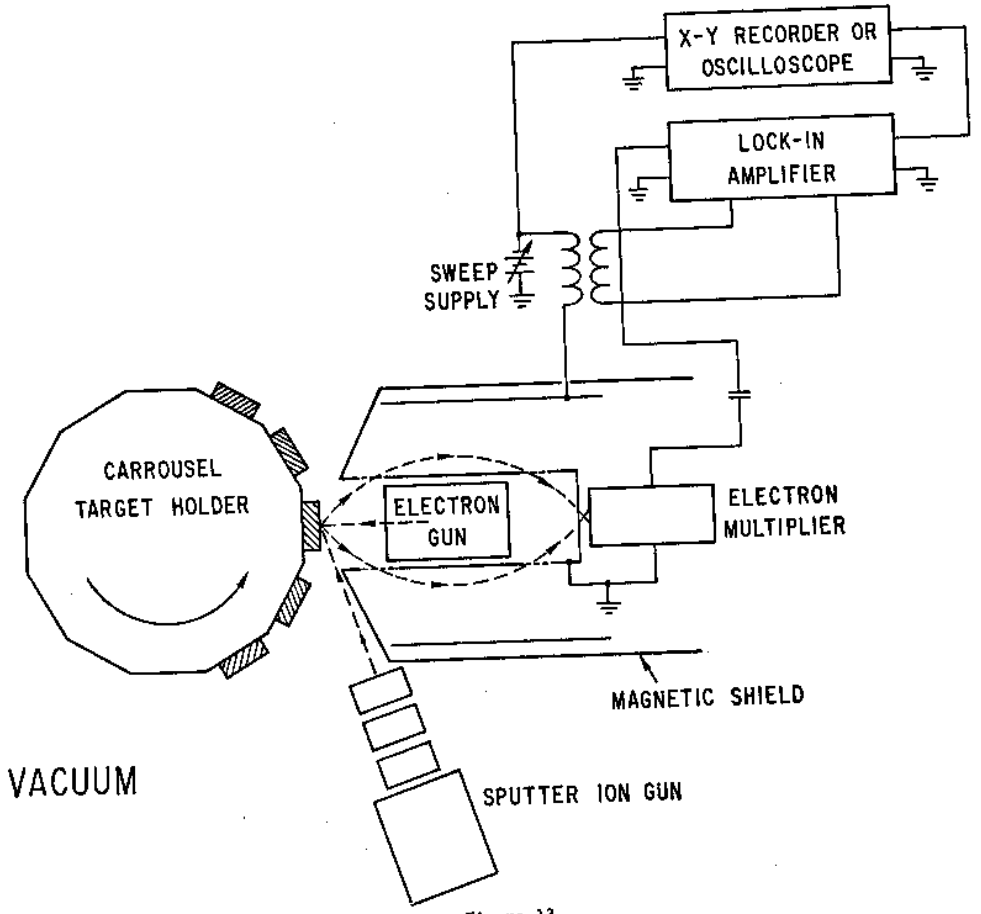
X-Y RECORDER OR
OSCILLOSCOPE
LOCK-IN
AMPLIFIER
SWEEP
SUPPLY
CARROUSEL
TARGET HOLDER
ELECTRON
GUN
ELECTRON
MULTIPLIER
MAGNETIC SHIELD
VACUUM
SPUTTER ION GUN

Figure 13

next specimen. An electron gun within the inner cylinder directs a beam of electrons (depicted by dashed arrows) towards the specimen being analyzed. As the electron beam is accelerated towards the sample, Auger electrons are emanated in all directions away from the sample. Some of these electrons can pass through two open slits. (Only those electrons able to pass through the slits are shown in this diagram; they are represented by dashed arrows). The open slits are positioned such that only those electrons which are bombarded off the sample at a certain angle (usually 42.3°)(76) are allowed through. The electrons which pass through each slit are then focused towards the electron multiplier. For every electron that reaches the electron multiplier, a count is recorded by the multiplier. In this way, the total number of electrons N(E) reaching the multiplier is recorded.

Focusing of the electrons passing through the slits occurs via the use of the sweep supply (located above the electron gun in Figure 13). The sweep supply provides a negative voltage to the cylindrical mirror shell. (The cylindrical mirror shell lies perpendicular to the specimen and so cannot be clearly seen. In order to view the electron gun an imaginary slice was made through the shell in Figure 13, so that the shell is now represented only by two lines. Each line lies within the magnetic shield lines. The upper line representing the shell is also shown as being connected to the sweep supply.) The negative voltage applied to the cylindrical mirror shell by the sweep supply repels the negatively-charged electrons. Consequently, by controlling the amount of negative voltage applied to the shell, the electrons can be repelled just enough to bend them back through the second set of open slits. As the electrons

pass through this set of slits they then hit the electron multiplier and are counted, as mentioned earlier. These electron counts are next amplified via the use of a lock-in amplifier and are finally recorded on an oscilloscope (see Figure 13). As the electron counts are recorded, the negative sweep voltage is recorded simultaneously. In this way, the energy distribution of the electrons can be obtained electronically by plotting the output of the electron multiplier versus the negative sweep voltage applied to the cylindrical mirror shell.(77) Having the energy distribution of the electrons, it is then possible to generate a plot showing the number of electrons versus the energy of those electrons. The plot shown in Figure 5 shows that unequal numbers of Auger electrons lie at each energy level.(78) The significance of this information will be explained in detail later.

The magnetic shield (shown in Figure 13 as two lines which lie just outside the two lines representing the cylindrical mirror shell) protects the system from the effects of other stray fields in the vicinity.

A vacuum throughout the spectrometer is necessary due to the nature of the electron beam. Electrons, such as those used to bombard the specimen surface, can travel only a few micrometers in air before they are stopped or slowed down by collisions with gas molecules.(79) In AES, such an occurrence would make specimen bombardment by an electron beam next to impossible. In fact, the development of Auger electron spectroscopy was hindered for many years until ultrahigh vacuum technology produced a vacuum system of between 10^{-7} to 10^{-10} Torr, which is the amount of pressure necessary for the interior of the cylindrical mirror analyzer to function.

The sputter ion gun (see Figure 13, bottom) has developed as one of the most useful auxiliary capabilities[80] in an Auger spectroscopic investigation of a material. The gun uses inert gas ion bombardment (generally argon gas)[81] to erode contaminated layers from the specimen surface in a relatively controlled fashion. The gun can be used in either of two ways. First, it can be used just before the Auger spectroscopy process commences in order to clean off contaminants which accumulated on the specimen surface while the specimen was being transported into the vacuum chamber. Since the sputter ion gun erodes the surface, this sputtering is a destructive process (in contrast to the non-destructive Auger process). This destructive nature of sputtering is used beneficially in its second type of application. If the ion beam and the electron beam are co-located at the focal point of the electron spectrometer, one can obtain an almost atom layer-by-atom layer profile (depth profile) of the chemical composition of the near-surface region of the specimen on a continuous basis.[82] Sputter rates of up to 3 Å/sec can be achieved for most materials using argon ions of 1,000-2,000 electron volts (1-2 keV).[83] It is also possible to automatically plot composition profiles using commercially available multiplexing instruments.

4.3 The Auger Process

It now becomes necessary to define the Auger process, and more specifically, the Auger electron at the atomic level. Figure 14 shows a schematic representation of a KLL Auger transition with electrons designated by solid circles and electron vacancies designated by open circles.[84] The uppermost figure represents a ground-state atom with two electrons in the K shell and eight electrons in the L shell. As the

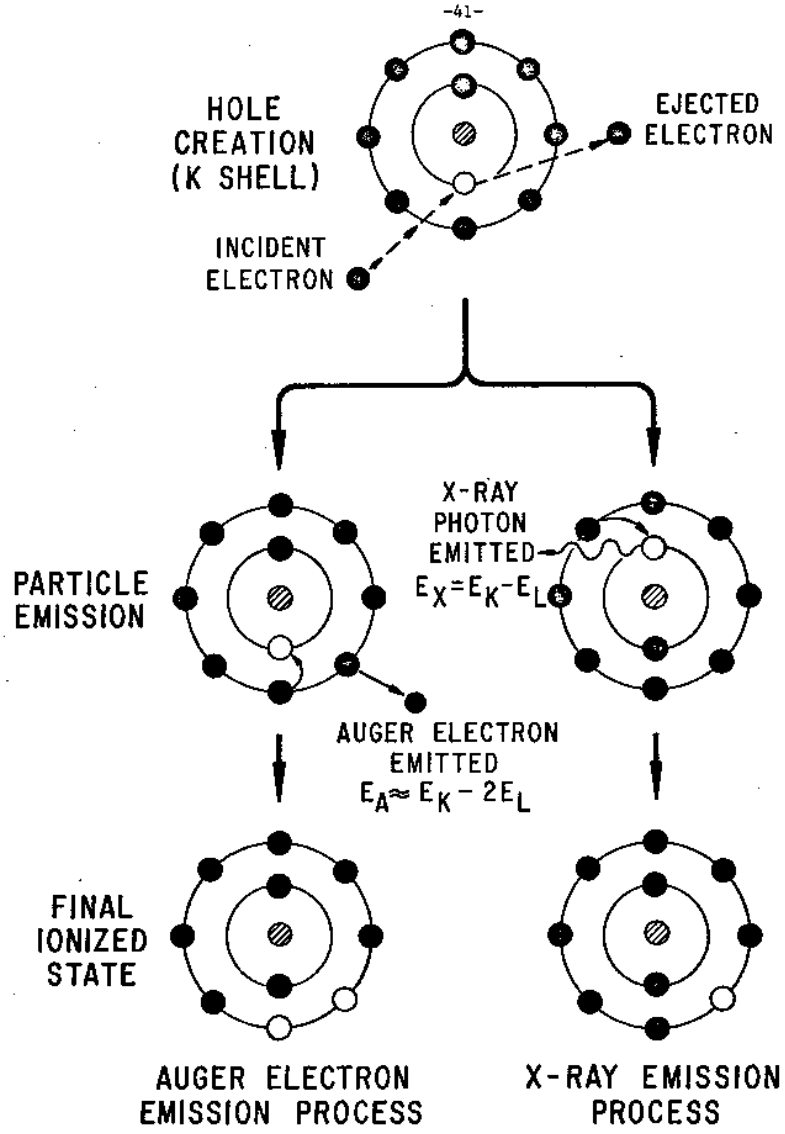
HOLE
CREATION
(K SHELL)
EJECTED
ELECTRON
INCIDENT
ELECTRON
X-RAY
PHOTON
EMITTED
$E_X = E_K - E_L$
PARTICLE
EMISSION
AUGER ELECTRON
EMITTED
$E_A \approx E_K - 2E_L$
FINAL
IONIZED
STATE
AUGER ELECTRON
EMISSION PROCESS
X-RAY EMISSION
PROCESS

Figure 14

specimen surface is bombarded with 1-5 keV of energy, an electron can be removed from the atom by the incident electron beam. This process only occurs when the binding energy of the core electrons is less than the kinetic energy of the electron beam.(85) If this condition exists, an electron of an inner shell (such as the K shell, as shown in Figure 14) is removed from the atom. A hole or vacancy is created in the inner shell as this electron is ejected. At this point, the atom is energetically unstable. To regain stability, an electron from a more shallow energy level now fills the vacancy left by the first ejected electron. It is useful to recall at this point that as an electron increases in its distance from the nucleus, it also increases in the amount of energy it possesses.(86) Therefore, as the second (more shallow, higher energy) electron fills the vacancy left by the first electron, excess energy is given off. This excess energy can be released in the form of an X-ray photon. In this case the electron would momentarily fluoresce and would possess an amount of energy E_X equal to the energy possessed by the K shell electron minus the energy possessed by the L shell electron ($E_X = E_K - E_L$). Alternately, however, the excess energy can instead be given to yet another (third) electron. If the third electron possesses enough excess kinetic energy, it will be ejected from the atom. This electron is known as the Auger electron. Referring back to Figure 13, it can again be noted at this point that when the Auger electron is emitted from the surface of the specimen, it enters the vacuum of the spectrometer and may be counted by the electron multiplier, providing it approaches the slit opening at the proper angle. In the vacuum chamber, the energy of this ejected Auger electron can also be measured and then identified with that of a specific element.

It is interesting to note here that the third (Auger) electron may either originate in the same energy level as the second electron (labeled "Final Ionized State" in Figure 14) or, alternatively, the Auger electron may originate in a more shallow (higher energy) level. This latter process is depicted in Figure 15 in an adaptation of a drawing by Riviere.[87] This process depicts the same sequence of events as does Figure 14; the style differs slightly between the two, but the main difference lies in the origin of the Auger electron. By convention, each transition is named by the electrons which relocated.[88] Therefore, Figure 14 depicts what is known as a KLL transition, while Figure 15 depicts a KLM transition. For the KLL transition of Figure 14, the energy of the Auger electron E_A equals the energy possessed by the K shell electron minus the energy possessed by two L shell electrons ($E_A = E_K - 2\ E_L$). For Figure 15, the energy of the Auger electron EA equals the energy possessed by the K shell electron minus the energy possessed by the L shell electron minus the energy possessed by the M shell electron ($EA = E_K - E_L - E_M$).

4.4 The AES Analysis Technique

As mentioned earlier, the plot shown in Figure 5 demonstrates that the Auger electrons bombarded off the specimen surface possess different amounts of energy, depending upon what transition type occurred (KLL, LMM, etc.). Specifically, the lower curve in Figure 5 represents the number of electrons N(E) having a certain energy E, in electron volts. As a beam of electrons with an energy E_P (here P = 1000 eV) strikes the surface of the sample (in this case, carbon), Auger electrons are reflected from the surface at energies ranging from zero to E_P (1000 eV). As Figure 5 shows, the number of electrons at each energy level is unequal.

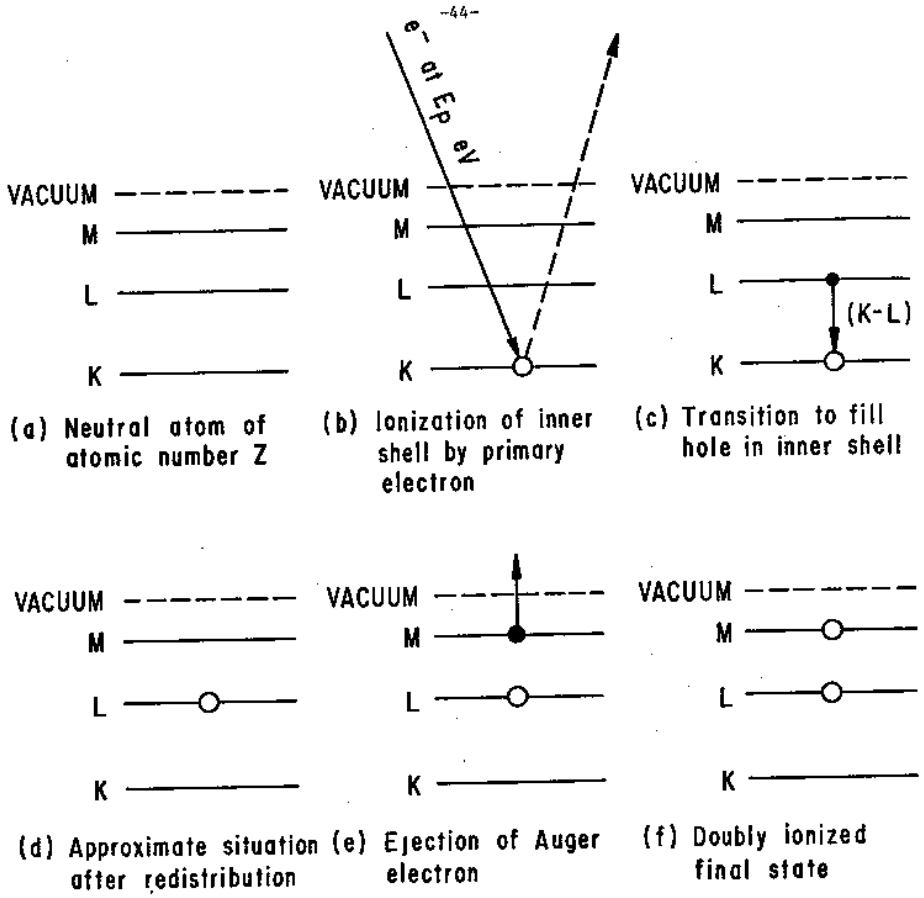

STEPS IN THE AUGER PROCESS FOR A SINGLE ATOM. TRANSITION IS KLM BY CONVENTION.

Figure 15

One peak of electron energies occurs at 1000 eV; this peak represents electrons which were reflected from the surface with no loss in energy whatsoever. These electrons always possess the same energy Ep as the incident electron beam (in this case 1000 eV), and the peak they create is known as an elastic peak. Figure 5 shows the presence of a peak just below the elastic peak; representing electrons scattered from the carbon surface after losing fixed amounts of energy, this peak is known as the plasmon peak. At the energy range 75-200 eV, electrons produced by a cascade process within the solid form a broad peak known as a true secondary peak. Such peaks as the elastic, plasmon, and true secondary peaks occur as a result of the Auger process but are useless in determining elemental composition of the sample and so are usually ignored.[89] They are mentioned here only to contrast their behavior with the behavior of important Auger peak(s).

In the case of carbon, the peak necessary for elemental analysis is the one which appears at 258 eV. This peak is distinguishable from other nonessential peaks (elastic, plasmon, true secondary) in that it occurs at a relatively fixed energy. For example, if the incident electron beam energy Ep was increased to 2000 eV, the elastic, plasmon, and true secondary peaks would move along the energy axis accordingly. The peak located at 258 eV, however, would not move considerably. It is this ability of certain Auger electrons to occur at relatively constant energy levels for each element which is used in a method to identify elemental composition. By performing AES on pure samples, characteristic peak locations can be recorded. An unknown can then be analyzed and its peak locations compared with those of pure samples until matches can be

made and an elemental composition determined. As mentioned earlier, instrumentation is available which can perform this process automatically as the unknown is analyzed.

It should be mentioned here that for purposes of simplicity, the actual energy distribution for a carbon specimen has been modified by this author in order to simplify explanation of the data. Keep in mind that carbon has more than one Auger peak which is used in elemental analysis as do most other specimen samples (see Figure 5).

It is interesting to note here that a theoretical approximation of the energies at which Auger electrons will appear can also be obtained using certain complex formulations. Persons interested in obtaining such formulations may refer to the article by Riviere listed at the end of this report.

To effectively reduce the background peaks (such as elastic and plasmon peaks) upon which the Auger peaks are superimposed, it is often convenient to electronically differentiate the N(E) function with respect to E (see Figure 5, upper curve). This is accomplished by applying a small AC voltage on the DC energy selecting voltage while synchronously detecting the output of the electron multiplier.[90] As shown in Figure 5, this has the effect of removing the background from the carbon peak and making the Auger peak easier to detect.

4.5 Conclusions

In conclusion, although Auger electron spectroscopy is a relatively new tool in the field of metallurgy and chemistry, it has several potentially valuable uses. Some areas of interest in which AES studies are

useful are corrosion, alloy formation, catalysis, thin film growth, and surface chemical interactions. One of the present major uses of AES is the detection and identification of impurities at grain boundaries of metals.[91] With sufficient stimuli, the technique of AES will hopefully become increasingly useful in laboratories, and occupy a role comparable in importance to X-ray diffraction and microprobe analysis.

5.0 THE INFLUENCE OF SURFACES ON THE BEHAVIOR OF SOLIDS

5.1 Introduction

Modern technology depends on the special properties of certain solids for the satisfactory performance of manufacturing processes. For the most part, these special properties are the bulk properties, but for an important group of phenomena these properties are the surface properties.[92] The properties of solids in general can be divided into two groups:[93]

(1) mechanical properties, and

(2) electromagnetic properties.

Mechanical surface properties (such as the frictional behavior of sliding surfaces) depend on the attractive forces between atoms of surfaces in contact; these mechanical surface properties also depend on the bulk plastic deformation properties of materials.[94] (Plastic deformation involves a permanent change in the shape of a piece of metal, or in the constituent crystals, brought about by the application of mechanical force which causes the crystals to slide or glide along slip planes).[95] The plastic behavior of a solid is much influenced by its surface condition; surface irregularities produce stress concentrations which affect the initiation of deformation, and layers of foreign atoms on the surface can affect the development of deformation.[96] (Deformation is defined as a change of form under mechanical stress).[97] The lubrication of sliding surfaces is greatly affected by the adsorption of molecules of lubricant onto the surface. The greater chemical reactivity of the surface atoms of solids causes adsorption of different molecules or atoms onto the surface; such adsorbed atoms can react chemically with each other.[98]

While solids are conventionally distinguished from liquids by being classified as pieces of matter of fixed shape, this distinction becomes a matter of degree when the solid is at a temperature near the melting point.(99) At high temperatures, atoms of a solid take part in diffusional motion. Surface atoms can be much more mobile than the atoms in the interior of a crystal. Surface diffusion also plays an important role in crystal growth from the vapor phase. Atoms can condense on any part of the crystal surface and diffuse along the surface to growth sites where they are incorporated in the lattice.

The electromagnetic surface properties include the reflectivity (the quality of casting back light or heat)(101) and thermal emissivity (the ability of a surface to radiate energy)(102) for electromagnetic radiation of all wavelengths, and the thermionic and photoelectric emission of electrons from surfaces. The special properties of surfaces, such as reflectivity, depend on the differences between the bulk properties on either side of the surface.(103)

A free surface affects the electrical conductivity of metals in many instances.(104) Under normal circumstances, these effects can be ignored, but for very thin films and at very low temperatures, the effects become appreciable.(105) Surface effects can be especially important for semiconductors.(106)

On the atomic scale, the difference between the surface properties and the bulk properties of any given material is due to the fact that the surface atoms have a smaller number of neighboring atoms.(107) The smaller number of neighbors results in the surface atoms being less

tightly bound to the lattice so that there is some additional energy (the surface free energy) stored in the surface. For a crystalline material, different crystal surfaces have different atomic arrangements and therefore different properties.(108)

5.2 Modern Implications of Surface Effects

Recently, several factors have come together to focus scientists' attention and effort on the investigation of surfaces.(109) One of these factors is the role of surfaces in microelectronics. As microelectronic devices are made smaller and smaller, the fraction of atoms in the device which are close to the surface increases; consequently, the surface itself becomes increasingly important to the operating properties of the device.

Surfaces also play an important role in vapor deposition processes. Vapor deposition methods are used extensively in manufacturing microelectronic devices because complex patterns can be created in a single step.(110) The characteristics of the devices depend on the composition, homogeneity, perfection, and integrity of the deposited layers. These in turn depend on the condition of the surface during deposition:(111) the degree of cleanliness of the substrate surface before deposition, the roughness/smoothness of the surface during growth on an atomic or microscopic scale, the presence or absence of adsorbed species, the presence or absence of dust particles on the surface (which, when present, can cause the formation of "pinholes" in the layers), and so on.

Another factor contributing to the current interest in surfaces is the commercial availability of reliable ultrahigh-vacuum equipment that

can operate routinely in the 10^{-10} torr range (10^{-10} torr is equal to the pressure exerted by one ten-billionth of a millimeter of mercury).[112] In such equipment it is possible to maintain a clean surface for a reasonable period of time; consequently, this has led to the development of methods for cleaning surfaces and methods for monitoring surface cleanliness, both of which are necessary for reliable and reproducible surface studies.[113] The availability of clean surfaces has led to a proliferation of methods of studying surfaces.

A lack of theoretical understanding also contributes to the current interest in surfaces.[114] Many bulk properties of materials are understood, but this understanding is based on models which, for the most part, do not treat surfaces properly. Some scientists are therefore turning to surfaces as a fruitful field of study and are beginning to examine the role of surfaces and their effect on a wide variety of properties.

5.3 A Standard Surface Study Technique: Vapor Deposition

Vapor deposition is used in a wide variety of processes in microelectronics; it is used to grow oxide on silicon for electrical insulation and is also used to apply metal conductors, to make capacitors, and to make resistors.[115] The vapor deposition processes in use include several different types of reaction between a gas and a surface:[116] deposition, co-deposition (on the same material or on a different material), chemical reaction with the surface layer, single crystal deposits (epitaxy), polycrystal deposits, and amorphous deposits. The variety of processes is virtually unlimited.

Vapor growth processes can be divided into two broad categories:[117]

the vapor deposition of materials which have a sufficiently high vapor pressure so that they can be transported directly as a vapor, and chemical vapor deposition, in which a high vapor pressure compound is formed to transport the species to be deposited.

One of the greatest problems in vapor deposition is the condition of the substrate surface.(118) If the surface has been exposed to air, then there are likely to be any of several atmospheric species adsorbed on it, such as oxygen, carbon dioxide, water, and hydrogen. (Adsorption is the accumulation of atoms or molecules on the surface of a solid or liquid from the medium in the immediate vicinity of the surface.)(119) As an example, glass usually has many tens of monolayers of water adsorbed on it (a monolayer is one molecule thick). In addition, other species can be introduced onto surfaces during processing. Impurities in the bulk can also segregate to the surface.

As mentioned earlier, the adsorbed species may be grown over and trapped into the crystal by the growth process, or they may be able to diffuse on the surface or through the bulk sufficiently rapidly so that they can stay at the surface during growth. In either case, they can form a significant impediment to the growth process.

If the adsorbed species becomes trapped in the crystal during the growth process it can have adverse effects. A monolayer of impurity trapped in a 1000 Å (300-atom-thick) deposit corresponds to a 1/3 percent impurity level, which is intolerable for many devices.(120) This illustrates why ultracleanliness, high-vacuum systems and rapid deposition rates (to cut down the time available for adsorption) are necessary conditions in vapor deposition.

If a dust particle is on a surface during vapor deposition, it will cast a shadow in the deposited layer, leaving a hole in it. Such a "pinhole" in a conductor may be of little consequence, since it merely reduces the effective cross section of the conductor. On the other hand, a hole in an insulating layer can be disastrous if the conductor on top short-circuits through it to the conductor below.

5.4 Additional Surface Study Techniques

There are many processes besides vapor deposition in which adsorbed species are important.(121) Adhesion of one material to another, for example, depends on the chemical bonds across the interface between them. Two metals adhere well to each other if their surfaces are clean; this fact has led to the phenomenon of cold welding, which has been demonstrated in ultrahigh-vacuum systems and in space.(122) However, when metals which have been exposed to the atmosphere are brought into contact, the metal-to-metal bonds cannot form. Instead, the adsorbed species on one surface come into contact with the adsorbed species on the other surface, and adsorbed species, in general, do not adhere to each other. Chemical reactivity also can depend strongly on adsorbed species. For example, copper or nickel adsorbed on the surface of silicon greatly speeds the rate at which hydrochloric acid will attack the silicon.(123)

5.5 Conclusions

In summary, there is little doubt that many properties possessed by the bulk of the solid are surface sensitive.(124) The recent development of numerous materials analysis techniques can only help to determine what other properties are surface sensitive.

6.0 METHODS OF MATERIALS ANALYSIS

6.1 Introduction

As stated earlier in this report, it is necessary to use ultrahigh-vacuum systems in order to study clean surfaces and so isolate the effects of adsorption. In air, the adsorption on a surface occurs very rapidly. At ordinary pressures, a monolayer can form in a few billionths of a second.(125) In contrast, in an ultrahigh-vacuum system at about 10^{-10} torr it takes about an hour for a monolayer to form on the surface.(126) In the last decade or so that commercial vacuum systems capable of operating in the 10^{-10} torr region have become available,(127) it has finally been possible to maintain a clean surface long enough for experimental purposes.

New techniques that permit detailed investigation of many of the properties of surfaces have been developed over the past several years; Table 1 (shown on page 55) gives a list of the types of techniques available.(128) These techniques fall into three general categories, each providing a different kind of information about surfaces:

(1) techniques that provide an actual picture of the surface, formed by some direct imaging technique; this technique delivers topographic and geometric information about the surface,

(2) techniques that give information about the arrangement of atoms at the surface, using diffraction, and

(3) spectroscopic techniques that provide information about the chemistry and electronic properties of the surface, by an

METHODS FOR STUDYING SURFACES

Technique	Application
DIRECT IMAGING	
Field-emission microscopy	Show dependence on orientation of work function
Field-ion microscopy	Show positions of individual atoms in surface layers
Transmission electron microscopy	Show crystal structure of film; with replica technique, show surface topography
Scanning electron microscopy	Show surface topography
Scanning X-ray	Identify and show distribution of various species at surface
DIFFRACTION	
Low-energy electron diffraction (LEED)	Show arrangement of atoms to a depth of a few monolayers
High-energy electron diffraction (HEED)	Show arrangement of atoms near surface
SPECTROSCOPY	
Auger spectroscopy	Detect small quantities of foreign atoms on surface
X-ray microprobe	Identify species near surface
Ion-neutralization spectroscopy	Identify surface atoms and determine energy states
Ion bombardment	Detect and identify surface atoms
Positive-ion mass spectrometry	Identify trace elements in small volume
Infrared spectroscopy	Determine electronic configuration of surface atoms

Table 1

energy analysis of the interaction of ions, electrons, or light with the surface.

6.2 The Direct Imaging Techniques

As seen in Table 1, the direct imaging techniques include field-emission microscopy, field-ion microscopy, scanning electron microscopy, and transmission electron microscopy using surface replicas. In addition, the electron microprobe and a similar technique using ions can be used to give composition images of the surface.

The apparatus for field-emission microscopy is basically simple. First of all, the specimen is prepared in the form of a sharp tip.(129) This very fine tip is placed at the center of a glass sphere of approximately 10 centimeters diameter which has been coated on the inside with a fluorescent material.(130) The glass sphere is then pumped out and a potential is applied between the tip and the inner surface of the glass sphere. Electrons can be pulled from the tip and are then accelerated by the applied voltage to the fluorescent screen. The pattern that shows up on the fluorescent screen depends on the work function of the material (the work function is a measure of the ease with which electrons can be detached).(131) In vapor deposition studies made on tips of this nature, a few monolayers of a different species present on the surface could be detected by the change in the work function; this basic method has been extended to make the field-ion microscope.

The field-ion microscope is similar to the field-emission apparatus except that the electric field is reversed and the imaging is done by ionized gas atoms.(132) The gas atoms become ionized so close to the surface that the fields of individual atoms can be seen.(133) Once the

gas atoms have ionized, they accelerate rapidly towards the fluorescent screen; here they make an image which reveals the position of individual atoms on the tip. Grain boundaries and other defects can be seen and studied using this method. However, the number of materials which can be used for the tip is limited because the voltage necessary to ionize the gas atoms is almost enough to pull atoms from the tip. Most solids are not strong enough to withstand the high electrical fields required.

This effect can sometimes be turned to advantage; successive layers of atoms can be peeled off the tip by increasing the voltage slightly, thus revealing impurity atoms and vacant atom sites when they are at the surface of the tip.(134) The enormous magnifications which enable imaging of individual atoms are simply a result of the ratio of the tip radius to the viewing-screen radius.(135)

In transmission electron microscopy an image is formed by using magnetic lenses to focus electrons which have been accelerated through 50 kilovolts or more.(136) These electrons can penetrate a fraction of a micron into most materials.(137) Transmission electron microscopy gives significant information about the structure of thin films or other materials which have been "thinned," but only limited information about surface topography. However, replica techniques have been developed to reveal the surface structure. A thin layer of plastic or carbon can be deposited on the surface and then stripped off. This layer forms a replica of the surface which can be shadowed by evaporating gold or silver onto it at a low angle of incidence. The replica is then examined by transmission electron microscopy and reveals details of surface topography with a resolution of about 20 Angstroms.(138)

The scanning electron microscope also gives information about surface topography, but its resolution is limited to about 100 Angstroms.[139] The image is made by sweeping an electron beam across the surface of the sample in synchronism with a display beam on a cathode ray tube. The intensity of the electron beam in the cathode ray tube is controlled by the number of secondary electrons emitted from the surface. The image thus formed has much greater resolution and depth of field than an optical microscope image. Also, since the electron emission is greater, the image looks like a real picture of the surface.

A similar scanning technique, but one which uses the X-rays coming from the surface rather than the electrons, can make an image that shows the spatial distribution of various species at the surface.[140]

The resolution of an X-ray is usually significantly poorer than that of a scanning microscope, because the number of X-ray photons generated is small, but recent improvements in instrumentation have greatly improved the image quality.[141] An image of the surface showing the distribution of a chosen impurity can also be made by collecting secondary ions produced by sputtering.[142]

6.3 The Diffraction Techniques

Low-energy electrons are an ideal tool for studying surfaces on an atomic scale.[143] The technique using such electrons is known as low-energy electron diffraction, or LEED. LEED provides information about the surface arrangement of atoms. In LEED, low-energy electrons (on the order of 100 volts accelerating voltage) are directed onto a surface which is approximately one square centimeter in area.[144] The diffraction

pattern made by the coherently scattered electrons is observed. Since these low-energy electrons penetrate only a few atom distances into the crystal before they are scattered, an important part of the observed diffraction pattern comes from the atoms at the surface and displays the regularities in the surface arrangements.(145) A partial monolayer or a monolayer adsorbed on the surface will produce a diffraction pattern which shows the periodicity of the adsorbed layers superimposed on the periodicity of the substrate; however, several monolayers of adsorbed material will obliterate the surface pattern.

LEED is a sensitive method for observing adsorption on a surface and, because of this, imposes stringent requirements for surface preparation and cleanliness for reproducible results.(146) All LEED experiments must be done in ultrahigh-vacuum systems so that the surface will stay clean long enough for observations to be made.

The same kind of information can be obtained from high-energy electron diffraction, also known as HEED. HEED uses much more energetic electrons incident on the surface at a glancing angle. The path length of the electrons in the crystal is much longer, but if the incident beam is almost parallel to the surface, the penetration to the surface will be quite small and so the diffraction pattern comes primarily from the surface layers.(147) HEED can be particularly useful in examining bumps or particles on a surface; at glancing incidence, the electrons will reflect off the tops of the protrusions. The information that can be derived from these scattering events can be used to determine many chemical and physical features about the host material.(148)

6.4 The Spectroscopic Techniques

The spectroscopic techniques for surface analysis depend on the interaction of electrons, ions, or light with the surface. One of the most sensitive methods for obtaining information about impurity atoms on a surface is Auger spectroscopy;[149] this method is discussed in detail in Section 4.0 of this report. In Auger spectroscopy a monoenergetic electron beam (a beam consisting of electrons whose energies are within an extremely narrow range), with an average energy of about 3 keV,[150] is directed at the surface. The incident electrons excite the electrons of atoms in the solid, which then lose energy by transferring it to another electron; this is known as the Auger process. The Auger electrons escape from the surface if they are generated close enough to it. The energy distribution of the electrons which are knocked out of the surface depends on the species present within a few atom layers of the surface. The principle advantages of the Auger method are that it is non-destructive and may be used to determine properties of the material studied in a small area of that material.[151] The technique can be used to detect small quantities of foreign surface atoms.

The X-ray microprobe uses high-energy electrons (accelerated by 10 to 50 kV)[152] to irradiate a small volume of material near the surface. The X-rays coming from the surface identify the species present in the volume irradiated. This method can detect only fairly thick surface layers since the high-energy electron beam (it must have high energy to excite X-rays) penetrates at least one micron into the material.[153]

Ion-neutralization spectroscopy can be used not only to identify surface atoms, but also to determine the energy states of atoms at the

surface.[154] An ionized atom incident on the surface under a small accelerating voltage (4 to 100 volts)[155] produces electrons whose energy spectra can be analyzed to obtain information about the local density of states at the solid surface.

A chemical analysis of a surface can be obtained by an ion-bombardment technique. The surface is bombarded with relatively high-energy (100 to 2000 eV)[156] ions of a rare gas. The energy distribution of the backscattered ions depends on the mass of the surface atoms, and can be determined with a mass spectrograph. The penetration of the incident ions is sufficiently small so that small amounts of adsorbed impurity can be detected.

Positive-ion mass spectrometry, although basically a bulk rather than surface technique, analyzes only a small volume, and is very sensitive to trace amounts of impurity. A sensitivity of 10 parts per billion has been claimed for this new technique, which consists of sputtering atoms from a small area of the surface with oxygen or other ions at high energy (about 10 keV), and then analyzing the sputtered atoms with the aid of a sensitive mass spectrometer.[157]

Infrared spectroscopy looks very promising for the future, largely because of the development of high-energy lasers.[158] With it, the electronic configuration of the atoms on the surface can be detected. For example, it is possible with infrared to tell whether carbon and oxygen on the surface are present as separately adsorbed carbon and oxygen atoms, or whether they are joined together as CO molecules or CO_2 molecules.[159]

6.5 Conclusions

This impressive array of new techniques, many of which are possible only because of the advent of ultrahigh-vacuum systems, can give much detailed information about surface structures, surface species, and surface topography. However, all of these techniques are complex and require sophisticated instrumentation, very careful sample preparation, and a high degree of experimental ability. Seldom can more than a few of them be applied in the same apparatus to the same material.

These techniques hold the promise of being able to characterize topography and atomic arrangement, and to determine the species present at a surface and the electronic configuration of those species. This knowledge will be important for unraveling the complexities of the structure and properties of surfaces and surface states.

7.0 APPLICATIONS OF TECHNIQUES

7.1 Studies Performed Using Electron Spectroscopy for Chemical Analysis (ESCA)

7.1.1 Introduction to Electron Spectroscopy for Chemical Analysis (ESCA)

Electron spectroscopy for chemical analysis (ESCA) is also known as X-ray photoelectron spectroscopy.(160) This method involves the exposure of a sample of interest to a source of monochromatic X-rays, followed by analysis of the energy of the spectrum of emitted photoelectrons from the sample.(161) In this way the binding energies of the electrons in both the core and valence bands are measured. This information in turn provides information of a chemical nature about the bulk sample, and in particular about its surface.

As with related techniques mentioned earlier in this report (see Section 6.0), the experiments using ESCA must be performed in a vacuum. Samples are generally solids, but may be studied while in such forms as powders or frozen liquids.(162)

7.1.2 A Study of Fluoride-Treated Tooth Enamel Using Electron Spectroscopy for Chemical Analysis (ESCA)

Electron spectroscopy for chemical analysis (ESCA) has been used to study the chemical properties of different fluoride coatings on tooth enamel.(163) Depth-composition profiles of the fluoride coatings were obtained by measuring photoelectron peak amplitudes as a function of argon sputtering time.(164) Measurements of the binding energy of the photoelectron lines as a function of depth helps determine chemical

association. For example, binding energy measurements of the stannous fluoride coating in one tooth enamel sample under investigation showed that tin is primarily bonded to fluorine; this was also true for the photoelectron spectrum of the sodium fluoride coating in another sample under study.(165)

The depth profiles obtained for the samples under study demonstrated that it is possible to characterize enamel coatings as a function of depth.(166) In addition, the results of this particular study showed that the tooth enamel samples treated with sodium fluoride possessed a higher binding energy for sodium. The existence of this higher binding energy for sodium suggested that a stronger sodium-fluorine bond exists in these cases than in acidulated phosphate fluoride samples or samples treated with monofluorophosphate.(167)

The binding of certain compounds to tooth enamel is significant in that a certain milieu is created around the tooth; this milieu can either retard or encourage the growth of bacteria on the enamel. Most persons can attest to the destruction and eventual pain resulting from this adhesion of bacteria to enamel; the dollar cost of reversing the damage incurred to the teeth is reflected in dental bills. An insight into the important role ESCA and other surface analysis techniques play in such health fields as medicine, biology, and chemistry can be gained through familiarization with such studies as the one just discussed here.

7.1.3 Surface Analysis and Depth Profile Composition of Bacterial Cells Using Electron Spectroscopy for Chemical Analysis (ESCA) and Oxygen Plasma Etching

As mentioned earlier, electron spectroscopy for chemical analysis

(ESCA) (also known as X-ray photoelectron spectroscopy) gives the energy spectra of electrons that are photoejected by exciting X-rays from the surface layers of a specimen.(168) The spectra provide information about binding energy of the ejected electrons and therefore provide the elemental composition of the specimen surface. The surface depth so analyzed is on the order of a few nanometers.(169) Low temperature oxygen plasma etching oxidizes the surface layers of a specimen at temperatures below 100°C, etching away the organic matrix and leaving behind mineral oxides and salts of the exposed elements.(170) The morphological results of such etching can be ascertained using electron microscopy.(171)

A combination of surface analysis obtained by X-ray photoelectron spectroscopy and oxygen plasma treatment of biological specimens can therefore yield the elemental composition of the outermost surface as well as in-depth elemental profiles of the same specimens as etching progresses.(172) This rationale was applied to a study of the distribution of teichoic acids in the cell walls of Gram-positive bacteria, the nature of cations on the cell surfaces, the layering of the envelopes in Gram-negative bacteria and the macromolecular composition of the cell surfaces.(173) X-ray photoelectron spectroscopy was used to analyze the outermost (2-5 nm)(174) surface of bacterial cells. Elemental analysis of the cell surfaces in Bacillus subtilis 168 and Bacillus megaterium KM gave a strong signal attributed to teichoic acids; conversely, teichoic acid-less Micrococcus lysodeikticus had a very weak signal for teichoic acids.(175) Oxygen plasma etching combined with X-ray photoelectron spectroscopy and electron microscopy was used to

obtain depth profiles of the cell surfaces. Distribution of teichoic acid throughout the cell wall of the two Bacillus species was also demonstrated.(176) Results obtained in this study indicated that the atomic ratios (C:O:N) of the surface biopolymers essentially agreed with known surface compositions for the species studied.(177)

In investigations such as the one examined here, surface analysis techniques can be used to verify or challenge results obtained earlier using other analysis techniques. In this particular study, the verification of the presence of teichoic acids in the cell walls of the species examined is important for several reasons, two of which are as follows:

(1) Teichoic acids are important as specific cell-surface antigens of Staphylococcus, Streptococcus, Lactobacillus, and Bacillus species.(178)

(2) The presence of teichoic acids indicates a Gram-positive rather than a Gram-negative bacterium.(179) Each bacterium type differs radically from the other in structural features as well as in response to various microbiological tests.

The identification of a certain bacterium as either Gram-negative or Gram-positive thus provides a realm of information about the characteristics of that particular bacterium and also identifies how the bacterium compares in its characteristics with other known bacteria. This study again exemplifies the importance of surface analysis techniques in fields other than materials science.

7.2 Studies Performed Using Mass Spectrometry Combined with Modern Laser Technology

7.2.1 Introduction

In this microprobe analysis system, the laser beams are used to supply ionization energy for the ionization of the sample and are also used as focusing aids.(180) More specifically, the process occurs as follows:(181) A high power pulsed laser beam is focused onto the sample at a diameter of less than 1 μm by a high quality optical microscope which, at the same time, is used to observe the sample. By the interaction of the ultraviolet laser light and matter positive and negative ions are generated which are mass analyzed by the mass spectrometer. The process generates an extremely high data rate. The spectra are either output on a pen recorder or are transferred to a computer for further processing.

Many types of compounds and materials can be analyzed quickly using this process. Some examples include:(182)

(1) embedded tissue sections mounted on standard electron microscope grids,

(2) smears and thin layers of cells or bacteria grown on support material,

(3) powders deposited on microgrids,

(4) soluble compounds deposited on supporting film, and

(5) particles up to several mm in diameter.

Since this process is capable of analyzing several types of specimens, it has a wide range of applications. These include:(183)

(1) trace element analysis in microsamples,

(2) microprobe analysis of biologically active ions,

(3) analysis of particulate materials such as dust and aerosoles,

(4) non-volatile compound analysis,

(5) fingerprinting of bacteria and polymers by laser pyrolysis/ionization,

(6) compound tracing in tissues, and

(7) layer-by-layer analysis of specimens.

7.2.2 An Investigation of Calcium Stores in Retinas Using Mass Spectrometry/Modern Laser Technology

The concentration level of intracellular or extracellular calcium (Ca) strongly influences the light response of photoreceptor cells.(184) It could therefore be expected that a regulatory system within the retina exists to control the concentration of extracellular and intracellular Ca. Such a system would need large stores to be able to effectively accumulate excessive Ca or to supply it in the case of depletion. A mass spectrometry/modern laser technology system (described in Section 7.2.1) was used in a study to prove or disprove the existence of such Ca stores.(185) Likely candidates for these were the mitochondria, since they are known to be able to accumulate Ca in other systems.(186) In addition, there are large amounts of mitochondria densely packed within the inner segments of vertebrate photoreceptor cells.(187) In this investigation, sections of frog retina (0.1-1.0 μm section thickness) were examined using the process described in Section 7.2.1.(188) Figure 16(189) is a micrograph of a frog retina section before analysis, while Figure 17(190) shows part of the same section as shown in Figure 16 after analysis.

As was expected, structures containing exceptionally large amounts of Ca could be found; however, contrary to expectation, exceptionally high amounts of Ca could be detected in the black shielding pigment

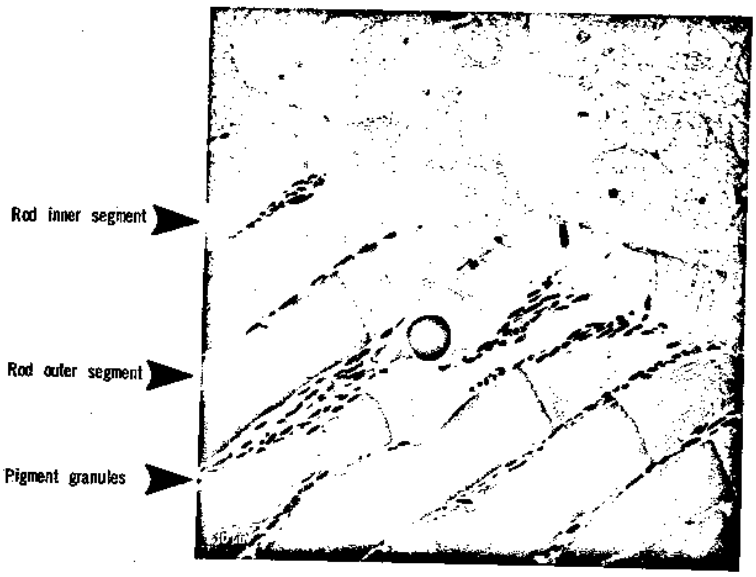

Figure 16

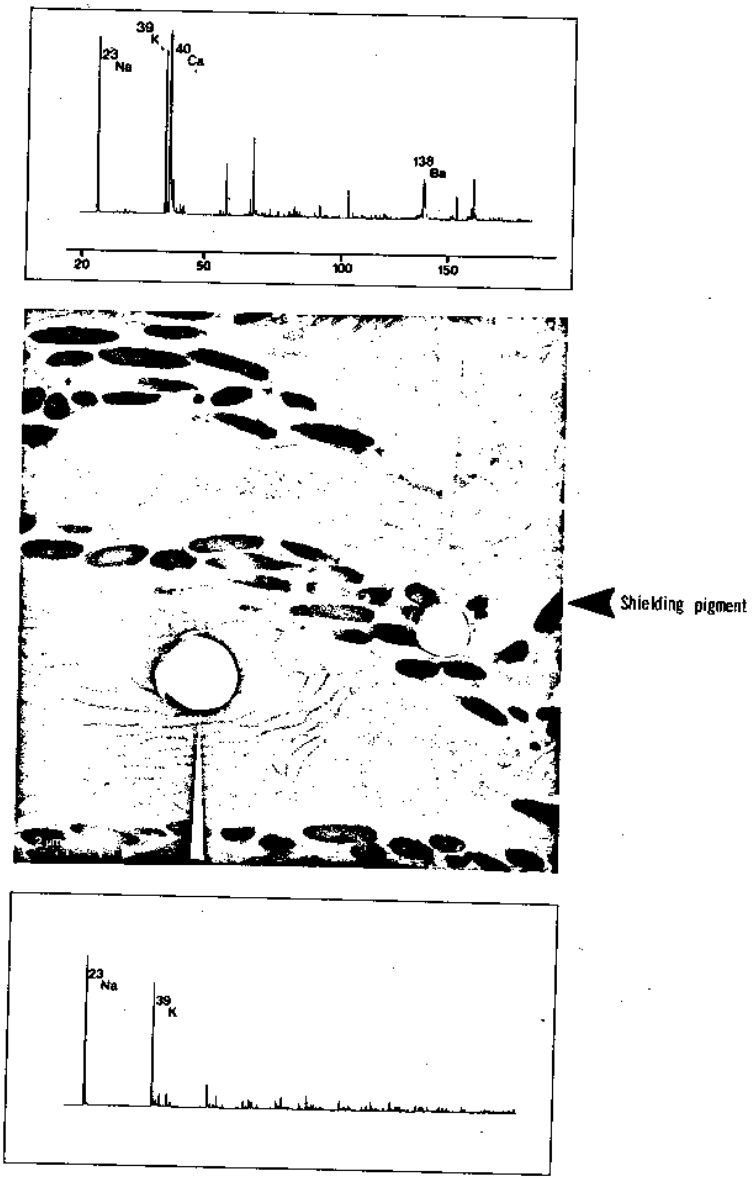
39
K
23
Na
40
Ca
138
Ba
20
50
100
150
Shielding pigment
2 µm
23
Na
39
K

Figure 17

(see Figure 17).[191] In the mitrochondria, a comparatively low Ca concentration was found.

As can be seen by comparison of the micrograph in Figure 16 with the micrograph in Figure 17 (taken from the same section before and after analysis, respectively), much information about the analyzed structures can be gained with electron-microscopic resolution.

7.2.3 An Investigation of the Localization of Ions in the Cell Wall Layers of Treated Wood

Since effective wood preservation is of high economic interest, knowledge of the effect of preservatives on wood is of great importance. In a study done on the effect of the solutions $K_2Cr_2O_7$, NaF, $CuSO_4$ and others on wood preservation, the main interest was to determine the distribution of the ions within the wood cells or cell walls.[192] The analysis using mass spectrometry/laser technology showed that in the pine wood section analyzed there is an irregular distribution of the ions along the cell walls; however, there is a significant preference for chromium compared with copper.[193] This can be clearly seen from a spectrum which was taken at a point within the cell wall (Figure 18).[194]

7.3 Conclusions

The value of surface analysis techniques to the materials scientist, biologist, chemist, dentist, or forensic physician is demonstrated by the volumes of knowledge which have been gathered through the use of surface analysis methods. Only a few examples have been mentioned here for purposes of brevity; however, many more combinations of techniques and applications of those techniques are in existence. It is the firm belief of this author that innumerable techniques are yet to be discovered.

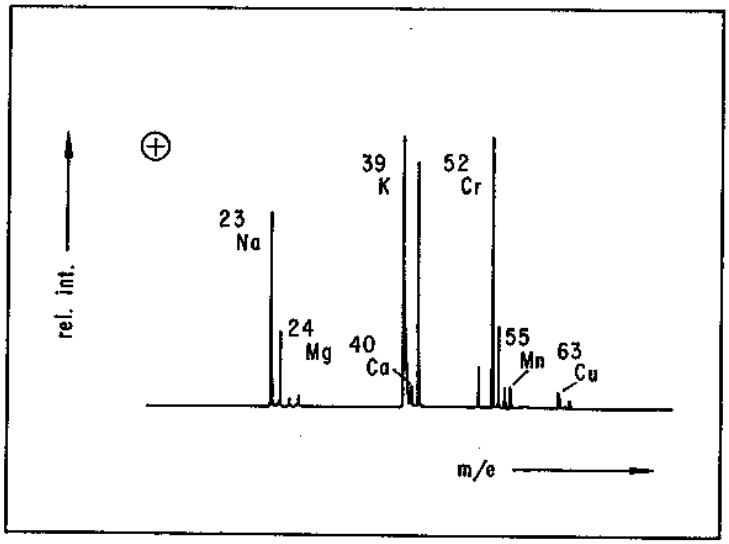

Figure 18

REFERENCES

1. ANL Document S3000-0001-AJ (October 1978). TREAT Upgrade (TU) and TU-Related Support Facilities Overall Plant Design Description. pp. 1-1.

2. Ibid.

3. ANL Document S3000-0001-AJ (October 1978). TREAT Upgrade (TU) and TU-Related Support Facilities Overall Plant Design Description. pp. 2-1.

4. ANL Document S3500-0001-AJ (April 1979). TREAT Upgrade (TU) and TU-Related Support Facilities System Design Description, Advanced TREAT Loop Systems. pp. v.

5. ANL Document S3100-0002-AJ (April 1978). TREAT Upgrade System Design Description, Mechanical Services. pp. 2-1.

6. ANL Document S3500-0001-AJ (April 1979). TREAT Upgrade (TU) and TU-Related Support Facilities System Design Description, Advanced TREAT Loop Systems. pp. v.

7. ANL Document S3500-0001-AJ (April 1979). TREAT Upgrade (TU) and TU-Related Support Facilities System Design Description, Advanced TREAT Loop Systems. pp. 1-2.

8. ANL Document S3500-0001-AJ (April 1979). TREAT Upgrade (TU) and TU-Related Support Facilities System Design Description, Advanced TREAT Loop Systems. pp. vi.

9. ANL Document S3400-0001-AJ (May 1978). TREAT Upgrade (TU) and TU-Related Support Facilities System Design Description, Modified Reactor Core. pp. 2-3.

10. Ibid.

11. Ibid.

12. ANL Document S3000-0001-AJ (October 1978). TREAT Upgrade (TU) and TU-Related Support Facilities Overall Plant Design Description. pp. 2-11.

13. ANL Document S3000-0001-AJ (October 1978). TREAT Upgrade (TU) and TU-Related Support Facilities Overall Plant Design Description. pp. 2-12.

14. ANL Document S3400-0001-AJ (May 1978). TREAT Upgrade (TU) and TU-Related Support Facilities System Design Description, Modified Reactor Core. pp. 2-1.

15. ANL Document S3000-0001-AJ (October 1978). TREAT Upgrade (TU) and TU-Related Support Facilities Overall Plant Design Description. pp. 2-13.

16. ANL Document S3000-0001-AJ (October 1978). TREAT Upgrade (TU) and TU-Related Support Facilities Overall Plant Design Description. pp. 2-12.

17. Ibid.

18. ANL Document S3400-0001-AJ (May 1978). TREAT Upgrade (TU) and TU-Related Support Facilities System Design Description, Modified Reactor Core. pp. 2-1.

19. ANL Document S3400-0001-AJ (May 1978). TREAT Upgrade (TU) and TU-Related Support Facilities System Design Description, Modified Reactor Core. pp. 2-2.

20. Ibid.

21. Ibid.

22. ANL Document S3400-0001-AJ (May 1978). TREAT Upgrade (TU) and TU-Related Support Facilities System Design Description, Modified Reactor Core. pp. 2-3.

23. TU Backup Core Design (2-13-80), D. Wade.

24. Personal communication (1980), A. Purohit, Argonne National Laboratory, Argonne, IL.

25. ANL Negative 113-79-276K (1979).

26. ANL Document S3820-0005-NS (October 1979). Statement of Work for Coated Fuel Can Test (CFCT). pp. 1.

27. Ibid.

28. Ibid.

29. ANL Negative 113-80-84 (1980).

30. Personal communication (1980), A. Purohit, Argonne National Laboratory, Argonne, IL.

31. Ibid.

32. Ibid.

33. Letter (5-17-79), K.V. Davidson, Los Alamos Scientific Laboratory, Los Alamos, NM, to M.J. Rieb, Argonne National Laboratory, Argonne, IL. pp. 1.

34. Ibid.

35. Ibid.

36. Ibid.

37. Letter (5-17-79), K.V. Davidson, Los Alamos Scientific Laboratory, Los Alamos, NM, to M.J. Rieb, Argonne National Laboratory, Argonne, IL. pp. 2.

38. Ibid.

39. Ibid.

40. Ibid.

41. Ibid.

42. Ibid.

43. Ibid.

44. Letter (5-17-79), K.V. Davidson, Los Alamos Scientific Laboratory, Los Alamos, NM, to M.J. Rieb, Argonne National Laboratory, Argonne, IL. pp. 3.

45. Ibid.

46. Weakley, B.S. (1972). A Beginner's Handbook in Biological Electron Microscopy. Northumberland Press Limited, Great Britain. pp. 66.

47. Personal communication (1980), A. Purohit, Argonne National Laboratory, Argonne, IL.

48. Dooley, G.J. III, and Haas, T.W. (1970). J. Metals, 22, 11. pp. 17-24.

49. Haas, T.W., and Pocker, D.J. (1974). J. Vac. Sci. Technol., 11, 6. pp. 1087-1092.

50. Thompson, M. (1977). Talanta, 24, 7. pp. 399-415.

51. Ibid.

52. Haas, T.W., and Pocker, D.J. (1974). J. Vac. Sci. Technol., 11, 6. pp. 1087-1092.

53. Ibid.

54. Personal communication (1980), A. Purohit, Argonne National Laboratory, Argonne, IL.

55. Thompson, M. (1977). Talanta, 24, 7. pp. 399-415.

56. Davis, L.E., MacDonald, N.C., Palmberg, P.W., Riach, G.E., and Weber, R.E. (1976). Handbook of Auger Electron Spectroscopy. Physical Electronics Industries, Inc., Eden Prairie, MN. pp. 5-11.

57. McGuire, G.E. (1979). Auger Electron Spectroscopy Reference Manual. Plenum Press, NY. pp. vi.

58. Letter (5-17-79), K.V. Davidson, Los Alamos Scientific Laboratory, Los Alamos, NM, to M.J. Rieb, Argonne National Laboratory, Argonne, IL. pp. 1.

59. Personal communication (1980), A. Purohit, Argonne National Laboratory, Argonne, IL. pp. 1.

60. Ibid.

61. Ibid.

62. McGuire, G.E. (1979). Auger Electron Spectroscopy Reference Manual. Plenum Press, NY. pp. v-viii.

63. Ibid.

64. Ibid.

65. Ibid.

66. Davis, L.E., MacDonald, N.C., Palmberg, P.W., Riach, G.E., and Weber, R.E. (1976). Handbook of Auger Electron Spectroscopy. Physical Electronics Industries, Inc., Eden Prairie, MN. pp. 5-11.

67. Ibid.

68. Ibid.

69. Courtesy of J. Balson (1980), Argonne National Laboratory, Argonne, IL.

70. Lyman, T., ed. (1948). Metals Handbook. American Society for Metals, OH. pp. 196-199.

71. Riviere, J.C. (1973). Contemp. Phys., 14, 6. pp. 513-539.

72. Stupian, G. (1974). In Systematic Materials Analysis, Vol. 1. Academic Press, NY. pp. 57-82.

73. Riviere, J.C. (1973). Contemp. Phys., 14, 6. pp. 513-539.

74. Palmberg, P.W. (1973). Anal. Chem., 45, 6. pp. 549A-556A.

75. Ibid.

76. Ibid.

77. Personal communication (1980), A. Purohit, Argonne National Laboratory Argonne, IL.

78. Riviere, J.C. (1973). Contemp. Phys., 14, 6. pp. 513-539.

79. Weakley, B.S. (1972). A Beginner's Handbook in Biological Electron Microscopy. Northumberland Press Limited, Great Britain. pp. 14-17.

80. Haas, T.W., and Pocker, D.J. (1974). J. Vac. Sci. Technol., 11, 6. pp. 1087-1092.

81. Thompson, M. (1977). Talanta, 24, 7. pp. 399-415.

82. Haas, T.W., and Pocker, D.J. (1974). J. Vac. Sci. Technol., 11, 6. pp. 1087-1092.

83. Ibid.

84. Courtesy of Physical Electronics Division, Perkin-Elmer Corp., Eden Prairie, MN.

85. Stupian, G. (1974). In Systematic Materials Analysis, Vol. 1. Academic Press, NY. pp. 57-82.

86. Drago, R.S. (1974). Principles of Chemistry. Allyn and Bacon, Inc., Boston, MA. pp. 98-136.

87. Riviere, J.C. (1973). Contemp. Phys., 14, 6. pp. 513-539.

88. Ibid.

89. Ibid.

90. Palmberg, P.W. (1973). Anal. Chem., 45, 6. pp. 549A-556A.

91. Dooley, G.J. III, and Haas, T.W. (1970). J. Metals, 22, 11. pp. 17-24.

92. Mykura, H. (1966). Solid Surfaces and Interfaces. Dover Publications, Inc., NY. pp. 1-4.

93. Ibid.

94. Ibid.

95. Shrager, A.M. (1961). Elementary Metallurgy and Metallography. Dover Publications, Inc., NY. pp. 373.

96. Mykura, H. (1966). Solid Surfaces and Interfaces. Dover Publications, Inc., NY. pp. 1-4.

97. Shrager, A.M. (1961). Elementary Metallurgy and Metallography. Dover Publications, Inc., NY. pp. 362.

98. Mykura, H. (1966). Solid Surfaces and Interfaces. Dover Publications, Inc., NY. pp. 1-4.

99. Ibid.

100. Ibid.

101. Barnhart, C.L. (1974). The World Book Dictionary. Doubleday and Company, Inc., IL. pp. 1739.

102. Barnhart, C.L. (1974). The World Book Dictionary. Doubleday and Company, Inc., IL. pp. 681.

103. Mykura, H. (1966). Solid Surfaces and Interfaces. Dover Publications, Inc., NY. pp. 1-4.

104. Ibid.

105. Ibid.

106. Ibid.

107. Ibid.

108. Ibid.

109. Jackson, K.A. (1972). Bell Lab. Record, 50, 6. pp. 181-188.

110. Ibid.

111. Ibid.

112. Ibid.

113. Ibid.

114. Ibid.

115. Ibid.

116. Ibid.

117. Ibid.

118. Ibid.

119. Ibid.

120. Ibid.

121. Ibid.

122. Ibid.

123. Ibid.

124. Machlin, E.S. (1962). In Strengthening Mechanisms In Solids. American Society for Metals, OH. pp. 375-404.

125. Jackson, K.A. (1972). Bell Lab. Record, 50, 6. pp. 181-188.

126. Ibid.

127. Riviere, J.C. (1973). Contemp. Phys., 14, 6. pp. 513-539.

128. Jackson, K.A. (1972). Bell Lab. Record, 50, 6. pp. 181-188.

129. Prutton, M. (1975). Surface Physics. Oxford University Press, Great Britain. pp. 57-61.

130. Jackson, K.A. (1972). Bell Lab. Record, 50, 6. pp. 181-188.

131. Ibid.

132. Ibid.

133. Bowen, D.K., and Hall, C.R. (1975). Microscopy of Materials. John Wiley & Sons, Inc., NY. pp. 248-270.

134. Ibid.

135. Jackson, K.A. (1972). Bell Lab. Record, 50, 6. pp. 181-188.

136. Weakley, B.S. (1972). A Beginner's Handbook in Biological Electron Microscopy. Northumberland Press Limited, Great Britain. pp. 5-14.

137. Ibid.

138. Jackson, K.A. (1972). Bell Lab. Record, 50, 6. pp. 181-188.

139. Bowen, D.K., and Hall, C.R. (1975). Microscopy of Materials. John Wiley & Sons, Inc., NY. pp. 13-66.

140. Jackson, K.A. (1972). Bell Lab. Record, 50, 6. pp. 181-188.

141. Ibid.

142. Ibid.

143. Farrell, H.H. (1974). In Systematic Materials Analysis, Vol. 1. Academic Press, NY. pp. 115-142.

144. Jackson, K.A. (1972). Bell Lab. Record, 50, 6. pp. 181-188.

145. Ibid.

146. Ibid.

147. Ibid.

148. Farrell, H.H. (1974). In Systemic Materials Analysis, Vol. 1. Academic Press, NY. pp. 115-142.

149. Jackson, K.A. (1972). Bell Lab. Record, 50, 6. pp. 181-188.

150. Ibid.

151. Forrest, P.G. (1970). Fatigue of Metals. Pergamon Press, Great Britain. pp. 175-204.

152. Jackson, K.A. (1972). Bell Lab. Record, 50, 6. pp. 181-188.

153. Ibid.

154. Ibid.

155. Ibid.

156. Ibid.

157. Bowen, D.K., and Hall, C.R. (1975). Microscopy of Materials. John Wiley & Sons, Inc., NY. pp. 71-73.

158. Jackson, K.A. (1972). Bell Lab. Record, 50, 6. pp. 181-188.

159. Ibid.

160. Proctor, W.G. (1974). In Systematic Materials Analysis, Vol. 2. Academic Press, NY. pp. 229-251.

161. Ibid.

162. Ibid.

163. Davis, L.E., and Riach, G.E. (1975). PHI Artworks No. 0223, 0224, 0225, 0226, and 0227. Physical Electronics Division, Perkin-Elmer Corp., Eden Prairie, MN. pp. 1-6.

164. Ibid.

165. Ibid.

166. Ibid.

167. Ibid.

168. Brundle, C.R. (1974). J. Vac. Sci. Technol., 11, 1. pp. 212-224.

169. Ibid.

170. Thomas, R.S. (1974). In Techniques and Applications of Plasma Chemistry. Wiley Interscience Publications, NY. pp. 255-346.

171. Ibid.

172. Millard, M.M., Scherrer, R., and Thomas, R.S. (1976). Biochem. and Biophys. Res. Commun., 72, 3. pp. 1209-1217.

173. Ibid.

174. Ibid.

175. Ibid.

176. Ibid.

177. Ibid.

178. Wheat, R.W. (1972). In Microbiology. Merdith Corp., NY. pp. 92-96.

179. Ibid.

180. Personal communication (1980), L.V. Phillips, Inficon Leybold-Heraeus, Syracuse, NY. pp. 1-15.

181. Ibid.

182. Ibid.

183. Ibid.

184. Ibid.

185. Ibid.

186. DeRobertis, E.D.P., Saez, F.A., and DeRobertis, E.M.F. Jr. (1975). Cell Biology. W.B. Saunders Co., PA. pp. 223.

187. Personal communication (1980), L.V. Phillips, Inficon Leybold-Heraeus, Syracuse, NY. pp. 1-15.

188. Ibid.

189. Ibid.

190. Ibid.

191. Ibid.

192. Ibid.

193. Ibid.

194. Ibid.